S04000000-TRT10000

ORNL/TM-2022/1843

SECOND TARGET STATION (STS) PROJECT

Detector needs for STS instruments

Anton Khaplanov

Date 2022-Jan-26

OAK RIDGE NATIONAL LABORATORY

MANAGED BY UT-BATTELLE FOR THE US DEPARTMENT OF ENERGY

ORNL/TM-2022/1843

SECOND TARGET STATION (STS) PROJECT

Document Number S04000000-TRT10000

Detector Needs for STS Instruments

Author(s)

Prepared by: Anton Khaplanov, STS Neutron Detector Lead
Name, Title

Approved by: Leighton Coates, STS Instrument Systems Science and Technology Manager
Name, Title

Date Published: Jan 26th 2022

Prepared by
OAK RIDGE NATIONAL LABORATORY
Oak Ridge, TN 37831-6283
managed by
UT-BATTELLE, LLC
for the
US DEPARTMENT OF ENERGY
under contract DE-AC05-00OR22

CONTENTS

CONTENTS iii
ABSTRACT 4
ABOUT THIS DOCUMENT 4
LIST OF ABBREVIATIONS 5
1. DETECTOR TECHNOLOGIES 6
  1.1 He-3 GAS DETECTORS 6
  1.2 SCINTILLATOR DETECTORS 8
  1.3 IMAGING DETECTORS 9
  1.4 DETECTOR BACKGROUND NOISE 9
2. STS INSTRUMENTS DETETECTOR REQUIREMENTS 12
  2.1 SPECTROSCOPY 12
  2.2 DIFFRACTION 14
  2.3 IMAGING 17
3. DETECTOR REQUIREMENTS COMPARED 19
  3.1 RATE ESTIMATIONS 19
  3.2 He-3 LINEAR POSITION-SENSITIVE DETECTORS 19
  3.3 SiPM ANGER CAMERA 20
  3.4 SiPM PIXEL CAMERA 21
  3.5 IMAGING DETECTORS 21
4. DETECTOR R&D NEEDS 23
  4.1 HIGH RATE FOR REFLECTOMETRY 23
  4.2 HIGH RESOLUTION FOR IMAGING 25
  4.3 MULTI-TUBE DETECTOR FOR BWAVES 27
  4.4 VACUUM-COMPATIBLE ANGER CAMERAS 29
  4.5 HIGH-RESOLUTION ANGER CAMERA 31
5. NEUTRON BEAM MONITORS 34
  5.1 BEAM MONITOR PERFORMACE ISSUES 34
  5.2 BEAM MONITOR R&D 35
  5.3 NEUTRON CAMERAS 37
6. DETECTOR R&D MILESTONES 38
  6.1 SiPM PIXEL DETECTOR 38
  6.2 IMAGING DETECTOR 39
  6.3 MUILTI-TUBE DETECTOR 40
  6.4 VACUUM ANGER CAMERA 41
  6.5 HIGH-RESOLUTION ANGER CAMERA (SEMSANS) 41
7. REFERENCES 42

ABSTRACT

This white paper contains an analysis of the requirements for the detectors for the initial suite of neutron scattering instruments at the Second Target Station, STS. The detector technologies proposed are compared with the instrument requirements, in-house proficiencies and strengths, and where appropriate, expertise at other facilities. Where relevant, alternative detector options are proposed. The performance gaps between the current state-of-the-art and the required characteristics are identified and projects within the R&D program are proposed in order to close these gaps. Further, neutron beam monitor needs are considered in a similar light.

ABOUT THIS DOCUMENT

The goal of this document is to establish a course towards delivering detectors that will fulfill the requirements of the STS instruments. The document contains the following main sections:

1. DETECTOR TECHNOLOGIES describes relevant neutron detector technologies, including those proposed for the STS instruments, as well as technologies used on comparable instruments in other facilities and those that may be relevant as alternative options.

2. STS INSTRUMENTS DETECTOR REQUIREMENTS analyzes the requirements and challenges for the detectors on the proposed instruments for STS.

3. DETECTOR REQUIREMENTS COMPARED contrasts the current state-of-the-art with the performance requirements of the STS instruments.

4. DETECTOR R&D NEEDS lists the R&D projects needed to bridge the gap between current and required performance as well as to leverage improvements to instrument performance where possible.

5. NEUTRON BEAM MONITORS will be needed on all instruments. A strategy for a standardized suite of beam monitors is presented along with incremental R&D to take the most advantage of available monitor technologies.

At the time of writing, 4 instruments – CENTAUR, CHESS, PIONEER and QIKR – have entered the preliminary design phase. The remaining 4 instruments – BWAVES, CUPI2D, EXPANSE, and VERDI – have been selected for construction and will enter preliminary design early in CY22. Two additional instruments have been identified to continue into preliminary design – M-STAR and TITAN. This document considers the requirements for all 10 of these instruments.

The document is intended to be complimented by the instrument proposals, where the scientific cases of each instrument and high-level scientific requirements are presented.

LIST OF ABBREVIATIONS

ANSTO – Australian Nuclear Science and Technology Organization
ASIC – Application-Specific Integrated Circuits
CMOS – Complementary Metal Oxide Semiconductor
EDM – Electrical Discharge Machining
FPGA – Field-Programmable Gate Array
FTS – First Target Station
GEM – Gas Electron Multiplier
GID – Grazing Incidence Diffraction
GIINS – Grazing Incidence Inelastic Neutron Scattering
GISANS – Grazing incidence Small-Angle Neutron Scattering
HV – High Voltage
ILL – Institut Laue-Langevin
LLB – Laboratoire Léon Brillouin
LPSD – Linear Position-Sensitive Detector
MCP – Multi-Channel Plat
MT – Multi-Tube
MWPC – Multi-Wire Proportional Chamber
NScD – Neutron Science Directorate
ORNL – Oak Ridge National Laboratory
PET – Positron Emission Tomography
PET/CT – Positron Emission Tomography / Computed Tomography
PImMS – Pixel Imaging Mass Spectrometry
PMT - Photo-Multiplier Tube
R&D – Research and Development
ROC – Read-Out Card
RRM – Repetition Rate Multiplication
S/N – signal-to-Noise
SANS – Small-Angle Neutron Scattering
SE – Sample Environment
SEMSANS – Spin Echo Modulated Small-Angle Neutron Scattering
SiPM – Silicon Photo-Multiplier
SNS – Spallation Neutron Source
STS – Second Target Station
ToF – Time-of-Flight
WLS – Wavelength Shifting
WLS – Wavelength Shifting Fiber

1. DETECTOR TECHNOLOGIES

Many technologies exist for thermal and cold neutron detection. Here, the focus is on those technologies that most adequately address the requirements of the initial suite of instruments at the STS. A combination of robust and well understood detectors with a strategic choice of R&D projects is aimed to maximize the performance of each instrument. R&D in these areas will advance detector state-of-the-art and ensure continued leadership in these areas.

1.1 He-3 GAS DETECTORS

Detectors based on ^{3}He gas have long been a gold standard in thermal neutron detection. High capture cross section and compatibility with high-pressure operation result in high efficiency. The inert nature of the gas allows detectors to last for decades with no service. The low atomic number of helium helps with low gamma sensitivity. Tube and chamber ^{3}He detectors are common at neutron scattering facilities. While recent shortage in the availability of ^{3}He has limited use of this detector technology, ORNL has a supply of ^{3}He sufficient to provide for the projected needs of STS and the currently operational ORNL neutron sources.

1.1.1 Linear Position-Sensitive Detectors

^{3}He-filled linear position sensitive detectors (LPSD) are the most common detector type used in neutron scattering today. These are produced commercially as tubes with a circular cross section. Other tube geometries are possible as a custom design [Marchal 2021]. In either case, position sensitivity is achieved using a resistive anode wire where the charge collected due to a neutron interaction divides itself according to the position of the interaction and is read out at both ends of the tube simultaneously. The obtainable position resolution is about a factor 2 better than the diameter (or the smallest dimension) of the tube.

LPSDs are characterized by high reliability and long service, high detection efficiency and simple, modular coverage of large areas. The signal-to-noise ratio is high due to large neutron signals and very low sensitivity to gamma-rays [Khaplanov 2013] and fast neutrons [Mauro 2015]. Further, tube detectors have a relatively low material budget making it easy to control unwanted scattering – a further benefit to the instrument signal-to-background. The drawbacks of LPSDs are related to the significant charge collection time. This limits the ability to adequately process multiple simultaneous events and reconstruct their positions along the tube [Khaplanov 2017].

The above characteristics make LPSDs a great choice for instruments where neutron count rate is not extreme, the scattered neutrons are spread over a large area, modest position resolution is required, and where high signal-to-noise is essential.

1.1.1.1 Single-tube detectors

^{3}He cylindrical LPSDs (^{3}He tubes) are produced commercially in a range of diameters (from 8 mm (1/3 inch) to 25 mm (1 inch)) and lengths (from a few cm to 4m). They have virtually no external parts beyond a metal cylinder, making them ideal to tile large areas. Combined with performance advantages outlined above, this makes them ideal for CHESS, VERDI, EXPANSE, and TITAN.

The selection of an optimal tube aspect ratio is an area that requires an optimization effort. In case of especially large length for a given diameter care must be taken to evaluate the reliability and performance. The experience from instruments with extreme aspect ratios of ^{3}He LPSDs on LET, ISIS, where 4-m long 25-mm diameter tubes were used [Bewley 2011] and VULCAN at the FTS with 1-m long 8-mm diameter tubes indicate limits the practical and low-risk designs. Most of the instruments at FTS have ^{3}He tubes arranged into assemblies of 8 tubes, 8-packs, with associated front-end electronics mounted of the rear.

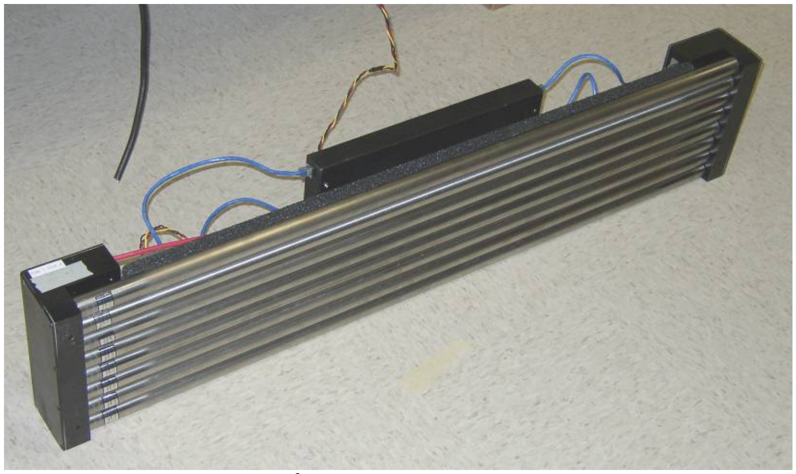

A ^{3}He detector 8-pack.

1.1.1.2 Multi-Tube detectors

The Detector Service Group at the Institut Laue-Langevin (ILL) has demonstrated the Multi-Tube detector technology [Marchal 2021] an alternative method of manufacturing LPSDs and has successfully implemented this technology at several ILL instruments as well as in Laboratoire Léon Brillouin (LLB) Australian Nuclear Science and Technology Organization (ANSTO). A single detector body contains multiple tubes sharing a common volume of ^{3}He. For larger detectors [Olivier 2006] this is achieved using steel tubes welded to common flanges. For tube lengths of 400mm and below, detectors have been machined from a monolithic block of aluminum using Electrical Discharge Machining (EDM).

The mono-block technique allows rectangular tubes, with a more uniform ^{3}He coverage of the detector surface and with narrower gaps than would be possible with circular tubes. Curved or flat detector geometries can be built with equal ease. The tube cross section can be chosen relatively freely. These considerations make the Multi-Tube a good match for the BWAVES requirements.

1.1.2 He-3 Chamber Detectors

To achieve higher position resolution than possible with LPSDs, while maintaining the excellent signal-to-background and efficiency of ^{3}He, a variety of chamber detectors can be built. Considering the detector dimensions and position resolutions needed at the STS, ^{3}He chambers are unlikely to be the preferred choice for the first 8 instruments. However, as a proven technology, ^{3}He chambers are worth keeping in mind in case of new requirements.

Chamber detectors are perfectly suited for curved (“banana”) detectors and have been installed on many diffraction instruments. The readout can be achieved either with the Multi-Wire Proportional Chamber method (MWPC) or with the Micro-Structured Gas Chamber method (MSGC). The detection principle is similar to tube ^{3}He detectors, however, here, anode wires, or micro-structured anodes are placed in a single gas volume, rather than individual tubes, often at a smaller pitch, resulting in higher position resolution.

A recent development is the Trench-MWPC [Marchal 2017], developed for “banana” or planar geometries, it maintains good position resolution of 2x2 mm^2, while overcoming the limitations of ^{3}He detectors in rate capability. Trench-MWPC detectors have been fabricated for 3 instruments at the ILL, which will be installed in 2022.

1.2 SCINTILLATOR DETECTORS

Scintillators have been effectively used at SNS and other facilities, notably ISIS and J-PARC, for diffraction instruments. They cover a gap where ^{3}He LPSDs lack position resolution, while high-resolution ^{3}He chambers lack coverage.

1.2.1 Anger Cameras

The Anger principle is based on sharing of scintillation light among clusters of pixel sensors. A transparent light-spreading layer is placed between the scintillator and the sensor. The signals from several adjacent pixels are combined to produce an order of magnitude higher position resolution than the pixel pitch. This technique has been used extensively in gamma imaging and has over the past decade been successfully implemented in neutron detection with the use of the GS20 ^{6}Li glass scintillator.

Earlier generations of Anger cameras used Photo-Multiplier Tubes (PMTs) as sensors, however, most future uses envisage Silicon Photo-Multiplier (SiPM)-based readout. The move to SiPM has improved position resolution to approximately 0.5mm and made the cameras highly resistant to magnetic fields – both valuable characteristics for the STS. [Riedel 2015]

Left: An SiPM Anger camera (with no scintillator mounted). Right: an array of 3 SiPM Anger cameras set up on DEMAND (HB-3A) at HFIR.

1.2.2 Pixel Cameras

Closely related to an Anger camera, a pixel camera variant does away with light spreading layer and uses finer sensor resolution that images the scintillator light directly. The scintillator is physically segmented to prevent light spreading. The result is a 1-to-1 correspondence of the location of a neutron interaction to a pixel. While giving up spatial resolution provided by the Anger method, the pixel camera can handle a far higher rate, since each pixel is immediately assigned as a neutron event, with no dead time in the rest of the detector.

This detector technique is now a standard in PET and PET/CT medical imaging. A challenge is to segment GS20 while keeping its thickness low-enough for a good gamma rejection characteristic. The NScD Neutron Technologies Detector Group has made progress in testing pixel detectors using GS20 scintillators. [Chong 2019, Chong 2021].

1.2.3 Wavelength-Shifting Fiber Detectors

An alternative type of neutron scintillator uses wavelength-shifting (WLS) fibers as a means of collecting scintillation light from either a large scintillator [Huq 2019], or a scintillator remote from the light sensor [Maliszewskyj 2018]. LiF:ZnS scintillators are typically used with WLS fibers. These emit more light than GS20, but are not transparent to their own light and have a large afterglow. Research into improved scintillators has shown that better scintillators are possible [Richards 2021, Sykora 2018, Wang 2015, Wang 2016)], and could potentially raise the count rate capability of WLS detectors.

1.3 IMAGING DETECTORS

Imaging detectors require both the highest spatial resolution as well as the highest rate capability of all neutron detectors. This had been typically achieved at the cost of the timing resolution and the ability to resolve individual neutrons using integrating detectors, such as image plates. Modern neutron imaging studies, however, require time resolution both to observe dynamic phenomena, as well as to resolve neutron time-of-flight (ToF) and thereby produce wavelength-dependent images.

1.3.1 Timepix/MCP Detectors

Imaging detectors based on the Medipix, or Timepix Application-Specific Integrated Circuits (ASICs) with a neutron-sensitive Multi-Channel Plate (MCP) converter have produced great neutron imaging results [Tremsin 2020]. Each ASIC has a limited area. The latest version, Timepix4 has an area of 28x28 mm^2, double the linear dimension of Timepix3. It further improves on its predecessor by offering the possibility to be tiled on all 4 edges. Further developments are needed in order to realize detectors using new ASICs to cover larger sensitive areas. The data acquisition chain must too be further developed in order to distinguish individual neutrons and their arrival times.

In most x-ray and charged particle detection applications, Timepix/Medipix ASICs are combined with a solid-state silicon sensor. It is attractive to implement this for neutron imaging, if a suitable neutron-sensitive semiconductor could be found.

An MCP can be readout with other techniques, for example using a delay line [Berry 2013]. However, it is difficult to approach the speed and throughput of a dedicated ASIC.

1.3.2 Imaging Cameras

An optical camera with a Timepix or CMOS sensor can be used to view a phosphorescent screen [Losko 2021]. Interchangeable optics can be used to adjust field-of-view and resolution. Cameras based on this principle have demonstrated ToF operation and sub-pixel resolution (ex. below 55um in Timepix).

1.4 DETECTOR BACKGROUND NOISE

Neutron scattering instruments often rely on a high S/N ratio in order to detect low intensity features. Therefore, sources of detector background must be minimized. This is achieved through both the design of the detectors, as well as through the design of the instrument and the detector environment.

1.4.1 Scattered Neutrons

The sample and detector area must be shielded from external and scattered radiation – thermal and fast neutrons and gamma-rays. Further, detectors must be protected from any scattered neutrons that do not originate from the sample. This includes (but not limited to) scattering in:

- Sample environment
- Multiple times in the sample, or sample and sample environment
- The gas (if any) between the sample and detector
- The detector housing
- The detection medium (ex. scattering from the quenching gas in a He-3 detector)
- The detector support structure or electronics

Shielding should be used to mitigate as many of these sources as possible. Unwanted scattering in the vicinity of the sample environment (SE) can be shielded by a radial collimator and shielding of the SE elements. Scattering in or near the detector – by shielding of all inactive elements and vanes between detector elements. While some materials, such as the neutron window of a detector cannot be shielded, measurement quality can be greatly improved using these principles.

1.4.2 Intrinsic Background

Background counts may originate in the detector itself. This can either be real radiation, electrical noise (discharges) or other false triggers.

Internal radioactivity

Some materials are naturally contaminated with radioactive isotopes, whose decay may be misinterpreted as neutron events. Notably, aluminum tends to contain trace quantities of uranium and thorium and their decay products [Khaplanov 2015]. The alpha decays from these are indistinguishable from neutron interaction and can constitute a significant background in very large detectors. For this reason, long LPSDs are best made from stainless steel, which does not have this issue. If a gas detector is to be made from aluminum, a worst-case background rate should be estimated and, if significant, a batch of Al with a sufficiently low contamination needs to be procured and validated. Other materials, for example tin, can also suffer from this issue.

False pulses/triggers

Pulses may be created in a detector with no ionizing radiation present. This can happen either due to contamination – ex. discharges in a gas detector (sparks); or due to induced electronic noise leading to triggers where no physical pulse was present. Incorrect grounding can be a major source of electronic noise.

1.4.3 External Background

External background may originate from other beam lines, directly from the target, from the accelerator, or from natural sources such as cosmic-ray generated neutrons. Reducing this type of background is not part of the detector R&D. Generally, shielding should be foreseen at the rear and sides of a detector in most cases. Coordination with the teams designing shielding and devices that constitute sources of radiation, is important while designing detector interfaces.

1.4.4 Prompt Pulse

Neutrons are created using a spallation reaction at high energy in the targets of both FTS and STS. This process is random, and while it does statistically liberate multiple neutrons per collision, it may less frequently result in nearly total energy transfer to a single neutron, proton or other particle travelling in a random direction (although predominantly along the proton beam axis). Such high-energy events, as well as spallation neutrons that enter the beamlines without being moderated, result in a signal in neutron detectors that is visible promptly after the proton pulse. This pulse begins immediately after the proton pulse and continues to drop off exponentially as fast neutrons randomly thermalize in the instrument cave and finally vanish.

The STS design of target, guides, shielding and instrument layout takes the prompt pulse into account and involves multiple techniques to suppress the effect [Zanini 2020, Santoro 2018]. Efficient shielding around the detectors will minimize the effect of fast neutrons that scatter and moderate in the cave which is typically composed of some form of concrete, shortening the tail of the prompt pulse. The design and material choices of a detector can further limit the sensitivity to fast neutrons [Mauri 2019].

1.4.5 Gamma Sensitivity

In a neutron scattering instrument the flux of gamma-rays may be significant, therefore, discrimination between neutrons and gamma-rays is essential. ^{3}He, and other gas-based detectors can achieve a gamma sensitivity on the order of a factor of 10^{-6}, or less relative to neutron efficiency thanks to the low gamma cross sections of the materials used and much longer tracks of Compton or photo electrons [Khaplanov 2013, Rossi 2015]. In scintillators, this is more challenging since the scintillator materials tend to have a sufficient density to stop Compton/photo electrons. Typically, a sub-mm scintillator thickness is needed to [Wang 2016] allow an efficient threshold rejection of gamma-rays. Some scintillators allow pulse shape discrimination [Wang, Riedel 2016].

2. STS INSTRUMENTS DETETECTOR REQUIREMNTS

2.1 SPECTROSCOPY

2.1.1 Detector Design for Spectroscopy

Neutron spectroscopy measures the energy transfer between scattering neutrons and a sample. The energies involved, ueV to eV, are far below the sensitivity of a particle detector, where detection processes liberate energy on the order of MeV. These small changes in neutron energy are determined by knowing the incident and scattered neutron energies. At a pulsed spallation neutron source, one energy is typically determined via an energy selection device like a neutron chopper or by Bragg scattering from a crystal and the other is determined from the neutron ToF. The time resolution of detection needed is on the order of 1us and is easily achievable by most detectors. Nevertheless, building detectors for spectroscopy is challenging. This is because very weak inelastic signals must be measured in the presence of strong elastic scattering, relying only on the detection time to discriminate the two. This is challenging because a small number of neutrons that undergo undesirable scattering in any component of the instrument, such as the sample environment, or the detector housing itself, can arrive with a delay due to their additional flight time. Other background sources can further contaminate measurements.

2.1.2 Direct Geometry Spectroscopy: CHESS

CHESS is a direct geometry cold neutron spectrometer. It is innovative in several ways. CHESS will measure a range of incoming energies in each frame, using the Repetition Rate Multiplication (RRM) technique. The resulting spectra are more complex, essentially being composed of a series of conventional spectra. While this is not an issue, it may become more difficult to handle the prompt pulse, which can appear at any point of the RRM spectrum, depending on energy settings. Care should be taken to suppress the prompt pulse as well as shorten its tail.

CHESS uses an innovative quasi-spherical detector configuration. This is different from the majority of ToF spectrometers, where a purely cylindrical array is used. For the detector technology, this does not present a challenge, however, there is an increase in complexity in the mounting structure of the detectors and access to the detectors. Shielding and radial collimation become more complex in this new layout. At the time of this writing, a classical cylindrical detector array is considered as an alternative.

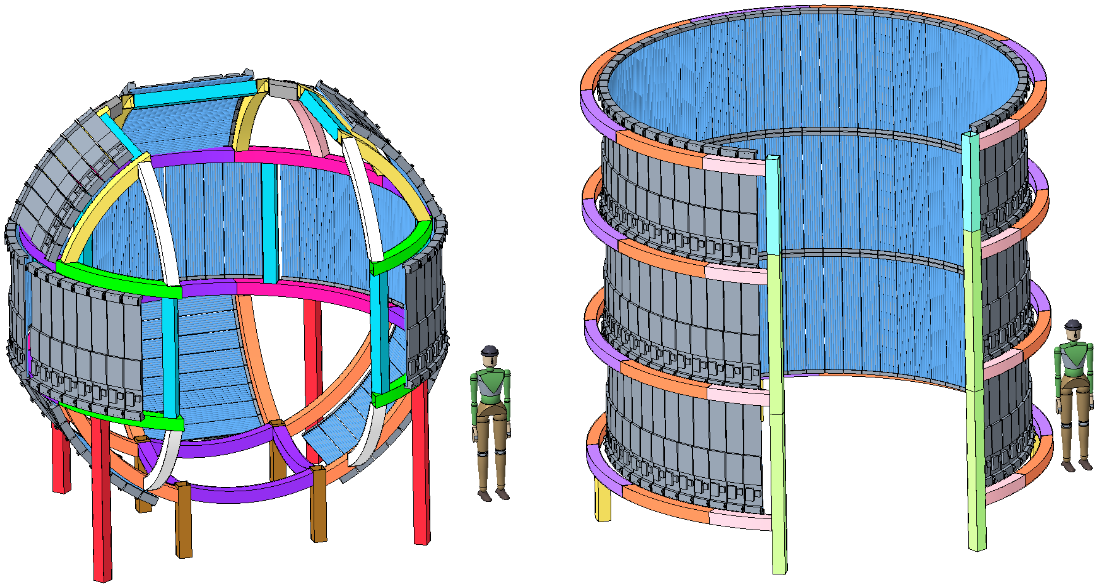

Detector array options for CHESS

The CHESS proposal includes a possibility of magnetic field coils placed in the vicinity of the detectors. Further, sample environments with strong magnets will be common. Therefore, the detector and readout must be validated to be insensitive to magnetic fields.

Conventional ^{3}He tubes are an adequate solution for this instrument. It is possible that the rate capability will not be sufficient to handle features such as Bragg reflections, however, these are typically not the features of interest. The ability to resolve very weak scattering at a very high signal-to-noise ratio, which is a typical strength of ^{3}He tubes, is far more essential. Improvements in the readout of ^{3}He LPSDs that may improve the rate capability will be sought where possible.

2.1.3 Neutron Spin Echo: EXPANSE

The EXPANSE proposal has rather moderate requirements for detectors. The solution based on short ^{3}He LPSDs arranged in two arcs in air is adequate and presents no major technological challenges, provided it is demonstrated that the stray magnetic field will not affect the performance. The greatest requirement is on the signal-to-background, where ^{3}He tubes are an optimal choice.

2.1.4 Indirect Geometry Spectroscopy: BWAVES

The BWAVES proposal describes a first-of-its-kind instrument within the inverse-geometry spectrometer class. It targets a final neutron wavelength much longer than any other instrument in its class – 14.5Å and longer. As no monochromator for this wavelength is available, a radial velocity selector, the WAVES device, is under development for this instrument.

The instrument is short, its experimental cave wedged between the neighboring guides. The detector and its vacuum vessel are restricted in diameter. The front-end electronics must be very close to the detectors. The back-end electronics may be further away, however, it is advantageous for the space and cable management, as well as for signal integrity to have them adjacent to the detectors. These requirements imply that the design of the entire vacuum tank, containing detectors the WAVES rotor, and the electronics must be efficient and compact.

Two options for the BWAVES detector exist: conventional ^{3}He LPSDs and ^{3}He Multi-Tube. The conventional round ^{3}He tubes would be 8mm in diameter. Multi-Tube detector would have rectangular ^{3}He tubes machined in a single block of aluminum. The rectangular tubes can be packed closer and have a more uniform depth than round tubes, resulting in better area coverage and uniformity. The detector depth can be decreased to 4 mm in the Multi-Tube option, halving the detector ToF contribution to the instrument energy resolution. The comparison between these two options is further detailed in the R&D section of this document.

Efficient shielding must be installed around the detectors. As a spectrometer measuring at a low intensity close to the neighbor instruments' guides, BWAVES is expected to require additional care in the design of its shielding.

2.1.5 Extreme Sample Environment: TITAN

TITAN uses large-area detector banks with detectors in vacuum flight chambers which do not extend all the way to the sample position. The sample environments will be especially large and include strong magnetic fields, possibly pulsed. The detector operation must be verified in these conditions.

Detector arrays composed of ^{3}He LPSDs address the detector coverage and signal-to-noise requirements adequately. The optimal configuration involves ^{3}He tubes that are 1.7 m long and 8 mm in diameter. This is greater than a standard aspect ratio and it must be verified that such a detector is reliable and does not compromise the performance. Larger tube diameters will be considered as backup and the instrument performance evaluated, possibly allowing ½ inch tubes to be used instead.

2.2 DIFFRACTION

Diffraction detectors measure neutron scattering angles. This information is used in combination with Bragg's Law to determine interatomic, or intermolecular distances within the sample. While older, reactor-based diffraction instruments usually relied on a monochromatic incoming beam, the STS instruments will measure ToF in order to determine the neutron wavelength.

Diffraction instruments are less sensitive detector background than spectrometers. Peaks with typically up to factor x100 variation in intensity are measured. Therefore, compared to spectroscopy, a higher noise baseline can be accepted, as can a higher pixel-to-pixel cross talk.

2.2.1 SANS/WANS: CENTAUR

The Small Angle Neutron Scattering instrument selected for the STS has a greatly extended angular range compared to most instruments in this class. It features detectors at 4 fixed positions – low, medium, large, and backscattering detector arrays. The position resolution required is 3x3mm^2, this is finer than most current SANS and cannot easily be fulfilled with He-3 LPSDs. The proposed solution is Anger cameras.

The detectors on CENTAUR will be stationary, therefore the typical cylindrical SANS vacuum vessel can be replaced with cone-shaped vacuum vessel segments where only the neutron flight path is evacuated. In this way, the detectors are placed at the vacuum boundary, and it is beneficial to evaluate possible advantages of detector in vacuum versus in air. In either case, most of the electronics must be in air in order to be cooled. The dimensions of the detector sensitive area will need to be larger compared to Anger Cameras currently in use. These aspects are further described in the R&D section.

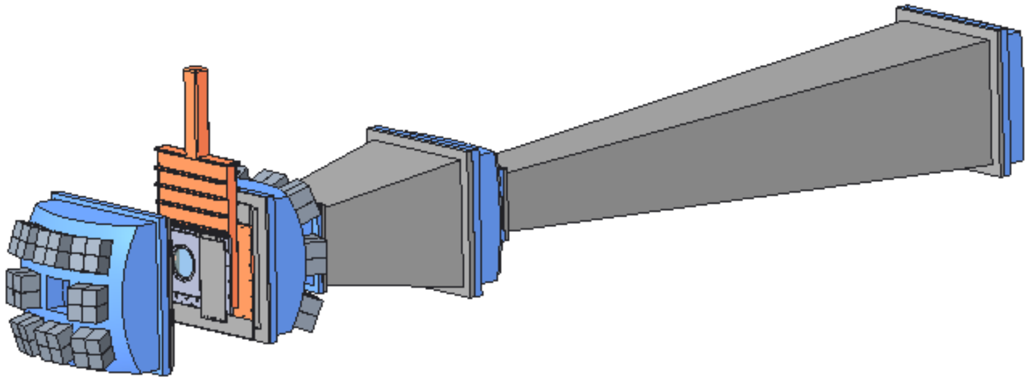

The vacuum tank and detectors of CENTAUR (work in progress). From left to right: backscattering detectors, sample area, high-angle, medium-angle, small-angle detectors.

Spin Echo Modulated SANS, SEMSANS, is one of the functionalities proposed for CENTAUR that requires a dedicated detector. SEMSANS detector measures a fringe pattern in the transmitted beam with a minimum position resolution of 0.2 mm. A dedicated detector would be required to fulfil this requirement.

2.2.2 Single crystal diffractometer: PIONEER

PIONEER aims to achieve close to 4pi detector coverage. The required position resolution is high – $0.6x0.6mm^2$, with a 0.8m sample-to-detector distance. To meet this high granularity requirement, Anger cameras are envisaged. The detector array will consist of a vertical cylindrical section and a removable bottom lid. On the order of 170 cameras are needed to tile both. This configuration allows space for large sample environment equipment. The detector array is not in vacuum; therefore, the current Anger Camera design will work. In order to balance the number of detectors with modularity of the array, an increase of the sensitive area of the current SiPM camera to approximately $150x150mm^2$ is envisaged. The resulting detector array has an area of approximately 3.8 m^2.

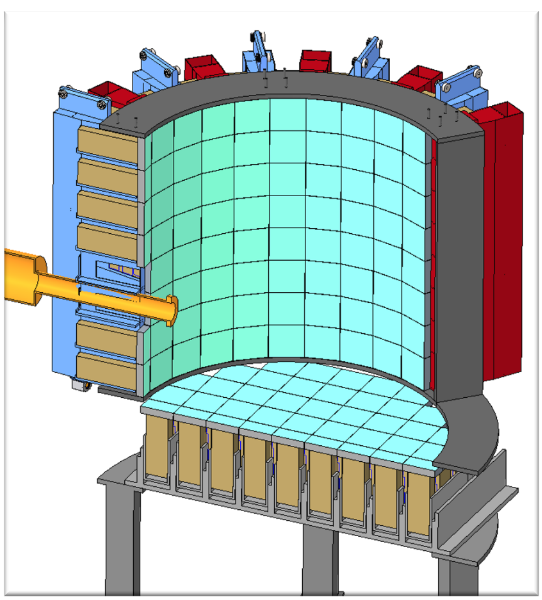

Cross section of the PIONEER detector array (work in progress).

2.2.3 Powder Diffractometer: VERDI

An optimal detector array for VERDI has a logarithmic sample-to-detector distance distribution with the backscattering detectors at 1.2 m and the forward detectors at 3 m. With this arrangement, the Q resolution varies smoothly and minimally for the range of scattering angles. The position resolution is compatible with conventional ^{3}He LPSDs. It is therefore natural to tile the detector area using 1-m tall tubes. The tube diameter will have to be chosen from 1/3 and 1/2 inch. While the thinner tubes offer a better position resolution, the thicker ones will have better efficiency, in particular for the lowest end of the wavelength range of 1Å. The layout of the sample-detector area of VERDI resembles that of the WISH instrument at ISIS, UK [Chapon 2011]. While detailed simulations of VERDI are not available at this time, we rely on the measured detector rates at WISH [Stefanescu 2017] and scale this with a factor of 10, corresponding to the expected increase in flux on sample. The resulting rates are well within the capabilities of conventional ^{3}He tubes.

2.2.4 Reflectometers

Reflectometers measure a neutron flux over a very large dynamic range. A typical reflectometry curve starts from a nearly total reflection at low Q and decays by over 6 orders of magnitude for large Q, while still carrying useful structural information about the sample. Furthermore, different levels of collimation may be used, increasing the dynamic range by a few more orders of magnitude. A detector must, therefore, cope a dynamic range of over 6 orders of magnitude.

Specular reflection is by far the most intense feature, impinging as an image of the beam onto the detector – a narrow stripe. The entire rate needs to be measured in only a few pixels. The pixel-to-pixel crosstalk must be very low, so that the intense specular signal does not contaminate off-specular scattering and other features.

The greatest rate challenge is the measurement of the direct beam. This is necessary in order to adequately normalize reflectivity data. Presently, no modern reflectometer is capable of measuring the direct beam. Attenuators must be used, and the real beam intensity reconstructed from a series of attenuator measurements.

2.2.4.1 Liquids Reflectometer: QIKR

QIKR is a reflectometer set up to measure horizontal surfaces, perfect for study of liquid-gas, or liquid-liquid interfaces. While in present instruments [Ankner 2008, Campbell 2011], beam deflection has been used in order to illuminate the liquid surfaces either from above or from below, QIKR avoids the compromises in beam quality this entails and instead features 2 separate beams each with its own sample-detector area. Each end station requires its own detector. The detector area is 200x200 mm^2, with a pixel size of 2x2 mm^2 at most, with a preference for 1x1mm^2.

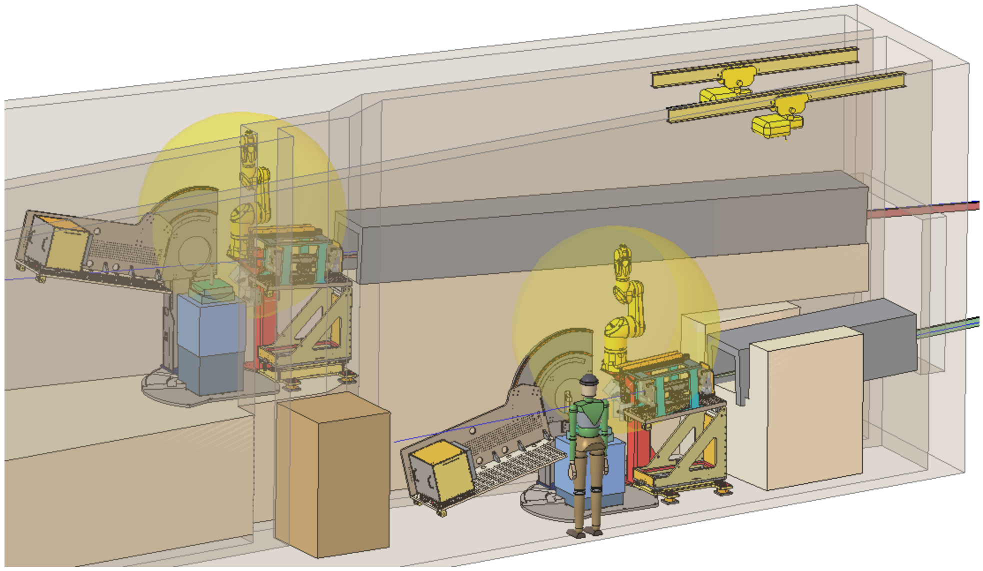

Layout of the QIKR double cave/experimental stations. Two equivalent detectors are needed.

2.2.4.2 Horizontal Reflectometer: M-STAR

M-STAR uses a vertical reflection surface, suitable for solid layers. The instrument aims to perform a range of complementary measurements together with classical reflectivity. These include off-specular scattering, Grazing Incidence SANS (GISANS), Grazing Incidence Diffraction (GID) and Grazing Incidence Inelastic Neutron Scattering (GIINS). In order to accommodate these additional options, a larger detector with a $500x500mm^2$ area with 1x1mm2 resolution and a very high count rate capability is required.
An additional diffraction detector is required for GID measurements at around 90° scattering angle with more moderate characteristics. This may be a pixel detector or an array of conventional Anger cameras.

2.3 IMAGING

Complementary to X-ray imaging, neutron imaging is highly sensitive to hydrogen, lithium and other light elements that are virtually invisible for X-rays. Likewise, many dense metals, that are opaque for photons, are transparent to neutrons.

2.3.1 Time-Resolved Imaging

Neutron cross sections are strongly dependent on the neutron energy and on the structure of the material. Therefore, selecting a neutron energy allows to image a specific element, or even isotope. While this can be done in monochromatic imaging, a far more powerful technique is ToF imaging where an entire neutron energy spectrum is used for imaging at the same time. The images at different energies are created by sorting neutrons by their ToF. This cannot be done with an integrating imaging technique, but only with an event-based readout with time resolution. Furthermore, time-resolved imaging enables imaging samples with dynamic behavior.

2.3.2 CUPI2D

An imaging instrument, such as CUPI2D, measures transmission, rather than scattering, in contrast to most other neutron instruments. Hence, the ability to detect the entire neutron beam on a small area is necessary – an extreme condition for a neutron detector. While previously, this has been solved using integrating detectors, time-resolved imaging requires either event mode or frame-based readout faster than is currently possible.

The time resolution needed to measure ToF is at most 1us, which is easily achievable by most particle detectors. The challenge is, however, to keep the event processing running with no bottlenecks or waiting times, so that each neutron can be assigned a correct timestamp by a system processing millions of events per second, including discrimination vs. gamma-rays, or multiple neutron detections. The imaging detector must not only cope with the detection but survive a high irradiation and a high pulse rate.

3. DETECTOR REQUIREMENTS COMPARED

In this section, the current capabilities of the detectors proposed for the first 8 instruments are compared to the current state-of-the-art with this type of detector.

3.1 RATE ESTIMATIONS

Rate capability is one of the key requirements that presents a challenge on several instruments due to the high flux of the STS. Estimated required rate capability is presented in terms of maximum time-average rate and maximum instantaneous rate.

The time-average rate does not take into account the temporal distribution of neutrons within a pulse, rather integrating the pulse structure. This figure is useful for estimating the data rate transmitted from the detector, that must be handled by the data pipeline, analyzed and stored.

The peak instantaneous rate is the maximum rate reached during the pulse. This is the key parameter that indicates whether the detector will suffer from saturation and loss of neutron counts.

In an ideal situation, a detector is able to handle the highest rate delivered by the beam line with negligible loss of counts. In practice, during high-rate peaks, saturation may occur, causing loss of counts during the peak. If no delayed dead time effects are present (such as afterglow, or data pipeline lag), such peak saturation may be acceptable if the features of interest are in the low-rate intervals during a pulse. In these cases, the time-average rate may describe the practical limitation more accurately than the instantaneous rate. This is typical for ToF spectroscopy, where elastically scattered neutrons result in a peak in the ToF spectrum that is many orders of magnitude larger than the intensity of inelastic scattering that is measured throughout the time frame.

The rate of incoming neutrons is also a measure of the radiation exposure of the detector. Detector components do suffer radiation damage and ageing effects that may or may not be recoverable. Extreme count rates may indicate the need additional design considerations for radiation hardness.

In the following, the time-average and instantaneous rates are presented per detector unit: **local count rate** and for an entire detector array: **global count rate**. The former characterizes the detector deadtime performance and the throughput of the front-end data acquisition, while the latter primarily the throughput of the data acquisition back-end.

A variety of estimates have been used for the values of rate in this section. Some instruments have progressed sufficiently at the time of writing and have access to simulated rates with worst-case scattering samples. In other cases, estimates have been made based on similar instruments at other facilities, scaled by the increase in flux at STS. Similarly, for some instruments, the ToF spectrum at detector has been simulated, which provides both time-average as well as instantaneous rates. In cases where such detail is not available, estimates were made based on the ratio of the peak flux and average flux.

Spatial distribution of the scattered neutrons is not uniform and depends on the type of sample used. For each local and global rate value, a worst-case scenario was considered. High global rate is typically caused by a strong incoherent scatterer, while a high local rate may correspond to a Bragg reflection where many neutrons are scattered into a narrow angular range. This means that there is no simple relation between local rate, global rate, the number of detector elements and detector area, rather, each rate value must be estimated individually.

All rates presented in the following are worst case rates.

3.2 He-3 LINEAR POSITION-SENSITIVE DETECTORS

The following table compares current to required parameters of ^{3}He LPSDs.

Parameter	Current	Required (CHESS)	Required (BWAVES)	Required (TITAN)	Required (VERDI)	Required (EXPANSE)
Sensitive Area (m^2)	-	33.8	0.37		15.2	2.13
Number of tubes		888	192	3570	1200	280
Shortest wavelength (Å)	-	1	14.5	1	1	4
Position resolution (mm^2)	4x1.5 (min)	25x25	10x2	12x12	12x12 Preferred: 8x8	25x25
Tube instantaneous rate (kHz)	50 (comfortable) 100 (possible) 150 (extreme)	150	10	10	50	5
Global instantaneous rate (kHz)	-	5000	100		6000	500
Tube average rate (kHz)	-	75	0.05	5	5	1
Global average rate (kHz)	-	2500	10		6000	100
Max background rate, total (Hz)		1	0.15			

3.3 SiPM ANGER CAMERA

The comparison of the currently achieved performance of SiPM Anger camera to that needed for PIONEER and CENTAUR. Each Anger camera operates with a global trigger – pulses are collected on all SiPM pixels when a neutron hits, meaning that there is dead time for the entire camera. For this reason, here, we do not consider pixel rate, but rather camera rate and global rate.

Parameter	Current	Required (PIONEER)	Required (CENTAUR)	CENTAUR SEMSANS	M-STAR GID detector
Total sensitive Area (m^2)	-	7.5	4	50x50mm2 +	0.25
Unit Sensitive Area (mm^2)	115x115	150x150	300x300	50x50	150x150
Number of units	-	170	37	1	3-15
Position resolution, (mm^2)	0.6x0.6 (0.35 with high-res SiPM)	0.6x0.6	3x3	0.2x0.2	0.5x0.5

Camera instantaneous rate (kHz)	1000	1000	100	100 000	100
Global instantaneous rate (kHz)	-	1000	100	NA (only 1 camera)	100
Camera average rate (kHz)	1000	100	10	10 000	10
Global average rate (kHz)	-	6000	2700 (wide angle detector) 5000 (all detectors)	NA (only 1 camera)	100
Max background rate (c/m^2/s)		100	10	NA	NA

3.4 SiPM PIXEL CAMERA

The following table compares the current achievements of SiPM pixel camera development with the requirements of the STS reflectometers. The SiPM pixel camera is an in-house R&D project and represents a promising option to address the requirements of reflectometers. Note that the very large rates here represent the measurement of the direct beam. The capability to do so is desirable, but not strictly required.

Parameter	Current	Required (QIKR)	Required (M-STAR)	Comment
Sensitive Area (mm^2)	20 x 20	200 x 200	500 x 500	Needed a tilable SiPM array.
Position resolution (mm^2)	2x2	1x1	1x1	Needed a SiPM with 1-mm pixels.
Pixel instantaneous rate (kHz)	>400	40 000	40 000	
Global instantaneous rate (kHz)	>4000	400 000	400 000	
Pixel average rate (kHz)	>200	20 000	20 000	
Global average rate (kHz)	>2000	200 000	200 000	
Background rate (Hz)	0.02 (He3)	0.1	0.1	

3.5 IMAGING DETECTORS

The following table shows the active area and spatial resolution for the CUPI2D detectors. The rate requirements are not shown, since the requirements is essentially “as much as possible”. Limitations will need to be identified during R&D and appropriate auxiliary detectors selected to fill the gaps.

Parameter	Current – Timepix/MCP	Current – Camera	Required – Timepix/MCP	Required – Camera
Sensitive Area (mm^2)	28x28	150+x150+	100x100	300x300
Position resolution (mm^2)	0.015x0.015	0.04x0.04 for 40x40mm^2 (variable FoV)	0.025x0.025	0.05x0.05

4. DETECTOR R&D NEEDS

This section presents detector R&D work needed to address several outstanding requirements for the 8 instruments under the construction scope of the STS. The proposed R&D topics are designed to mitigate the risk of not reaching the required performance and thus fully utilizing the increase brightness of the STS. Further, performance gains will be achieved in each case compared to currently available detector options.

4.1 HIGH RATE FOR REFLECTOMETRY

The ongoing development of SiPM pixel detector is expected to significantly enhance reflectometer detector performance and fulfill the requirements of rate and position resolution at QIKR as well as M-STAR. Rate capability with no appreciable dead time has been demonstrated up to 1.8MHz in a beam test on LIQREF at SNS [Chong 2021]. Adequate performance of the SiPM sensors and the readout chain is already demonstrated and understood thanks to their application in medical imaging. The combination with GS20 scintillator still needs further characterization of the ultimate rate capability and gamma-ray sensitivity. Performance should be evaluated in realistic reflectometry conditions and the effect of pixilation on the data understood.

4.1.1 Feasibility: SiPM Pixel Detector

The current prototype of the pixel detector uses commercial readout electronics. The segmented GS20 scintillator has been demonstrated down to 2-mm pixel size, however, additional work is required to decrease the pixel size to 1 mm. Further development will also be needed to better control gamma sensitivity.

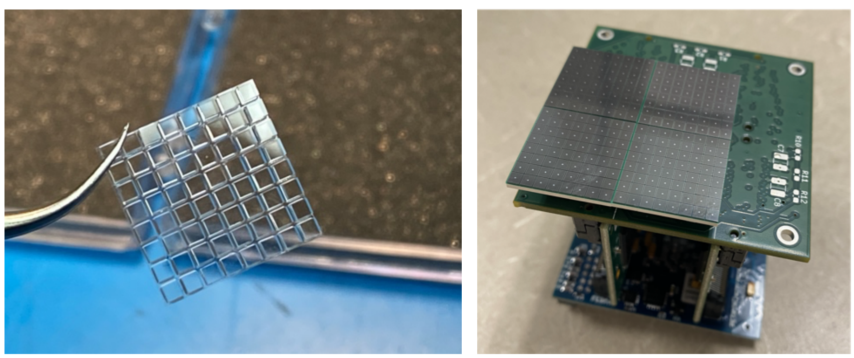

Pixel camera components. Left: segmented GS20 scintillator with 2-mm pixels. Right: Hamamatsu SiPM array with 2-mm pixel pitch designed to connect to the PETsys readout system.

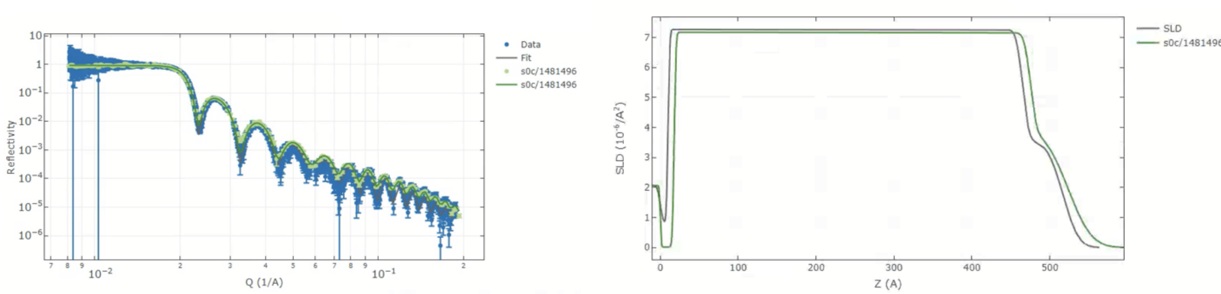

Left. Iridium reflectivity measured with the SiPM pixel camera on LIQREF at SNS. Right: corresponding SLD.

4.1.2 Risks: SiPM Pixel Detector

The count rate performance of the SiPM pixel camera appears relatively certain. More unknown are the efforts needed to achieve the necessary sensitive area, increase position resolution to 1 mm and decrease gamma-sensitivity. Other scintillator options may be considered [Richards 2021, Sykora 2018, Wang 2015, Wang 2016)] in the event of issues with pixelization of 1 mm, and if the required gamma insensitivity cannot be reached with GS20.

Performance risk

- Limitation of scalability of the sensitive area. a) cannot be scaled to $200x200mm^2$, b) cannot be scaled to $500x500mm^2$.
- Scaling results in detection non-uniformity.
- Mitigation: Backup solution for the larger M-STAR detector. Prototyping aimed at scaling specifically.

Schedule risk

- R&D requires significant effort in electronics engineering, fine machining of the scintillator and extensive testing.
- Mitigation: Ensure availability of technical and scientific personnel.

Budget risk

- Cost is currently unknown.
- Mitigation: Early prototyping of key components.

4.1.3 Opportunities: SiPM Pixel Detector

The new pixel detector will not only fulfill the requirements of the STS reflectometers. Reflectometers at FTS and essentially all other modern neutron sources would benefit from an improved reflectometry detector. As a detector based on the concept from medical imaging, where vast fluxes of photons are used, the pixel detector promises to essentially solve the rate limitation in reflectometry. It does so while maintaining high detection efficiency and position resolution. Other instrument types may benefit from the development as well, for example SANS or diffraction with high expected rates.

4.1.4 Back-up Solution: SiPM Pixel Detector

In the event a dedicated pixelated detector is not ready, a modified Anger Camera may be used. While the direct beam transmission measurement would not be achievable without attenuation, the direct flux can be estimated as done currently at FTS and the camera could provide all other measurements. The camera must be configured with a sufficient thickness of the light-spreading borofloat glass in order to shield the neutron-sensitive SiPM sensor.

The active area required for M-STAR, $500x500mm^2$, is a significant increase in area compared to $200x200mm^2$ on QIKR and will require additional development work. Alternatives should be considered, for large area of the M-STAR detector. One possible development is the Multi-Blade detector [Pisciteli 2018, Mauri 2020] that is planned to be installed on the ESS instruments ESTIA and FREIA [Andersen 2020]. This detector technology is new and its performance, including the final redout electronics, remains to be fully evaluated in its final version. If the design goal of the Multi-Blade of 2 orders of magnitude increase in count rate compared to ^3He chambers, is achieved, the Multi-Blade may present a viable alternative. It is expected to scale to $500x500mm^2$. A limitation of the Multi-Blade is the asymmetric position resolution (approximately 0.5mm x 2.5mm), which is adapted well to specular and off-specular reflectometry, but is not optimal for GISANS.

4.2 HIGH RESOLUTION FOR IMAGING

Imaging detector development is needed for both FTS and STS. The VENUS imaging instrument at FTS will need a sensitive area of 200x200mm^2, CUPID at STS – 100x100mm^2. Timepix/MCP detector is currently the most desired option. It has been demonstrated to be viable in terms of performance of each component, however, the R&D work needed to combine all elements into a detector of a required size is significant and needs to be pursued as a priority. The resulting detector will offer an unprecedented performance gain for the relatively large sensitive area of 100x100mm^2.

4.2.1 Feasibility: Imaging Detector

The Medipix/Timepix family of ASICs have proven highly capable for radiation imaging, including thermal neutrons. Even if the development does not advance beyond Timepix4, this chip already has the potential to fulfill the resolution and the count rate capability needed. It can also be tiled without a hard limitation that its predecessor had.

The neutron converter, MCP, with a diameter of up to 50mm has been demonstrated to work. It does however have known performance limitations related to uniformity and gain with increasing area. It has further limitations due to ageing. R&D is likely to address these issues, however, a considerable effort is needed. It is possible that the first generation of imaging detectors based on this technology will have limitations in uniformity and lifetime.

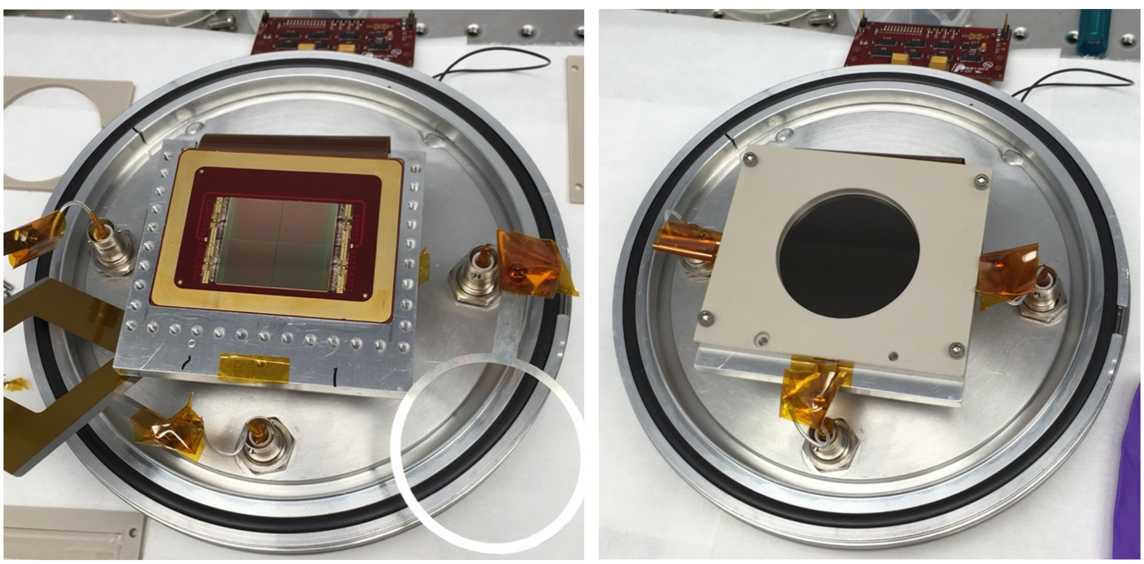

Components of a prototype imaging detector in their vacuum chamber. Left: a 2x2 array of Timepix3 chips. Right: Multi-channel plate (MCP).

4.2.2 Risks: Imaging Detector

Detectors based on Timepix and MCPs have been used in imaging and several related techniques over the past decade. However, a large technological advance is needed to meet the requirements of CUPID (and VENUS at FTS). Timepix4 is aimed at scalability, meaning that it is expected to perform as required when scaled to a 100x100mm^2 area.

Performance risk

- MCP cannot be reliably scaled to required area for technological reasons.
- Neutron-sensitive MCP cannot be procured due to lack of suppliers.
- Sufficient detection uniformity cannot be achieved for the active area required.
- Mitigation: collaboration with MCP manufacturer(s). Investigation of alternative neutron converters coupled to Timepix (this may be semiconductors).

Schedule risk

- Significant dedicated electronics engineering effort is required. Lack of a resource with sufficient skill level can delay the project.
- Mitigation: Allocate or hire an electronics and an FPGA engineer. Entry into the Timepix collaboration to ensure access to sufficient knowledge, failing this, outsource the work.

Budget risk

- Costs of MCPs (or alternative converters) are unknown, since these are currently not on the market.
- Project duration may increase, or additional project stages may be necessary.
- Mitigation: Collaboration with MCP/converter manufacturers. Entry into the Timepix collaboration to ensure access to sufficient knowledge.

4.2.3 Opportunities: Imaging Detector

The Timepix4/MCP detector has perhaps the best combination of the main neutron detector parameters up to date, except the active area. The scaling that will be needed for CUPID, is aimed at overcoming this limitation. With that, one can imagine future instruments with vastly improved fluxes operating all types of diffraction instruments with this detector, or a related technology (for spectroscopy, the gamma sensitivity is still likely to be a limitation).

The search for an alternative converter to the MCP, may be challenging, but if successful, could open entirely new possibilities by avoiding the size limitations of MCPs, vacuum requirements, and bulky detector edges.

4.2.4 Back-up Solution: Imaging Detector

The Timepix/MCP detector is expected to best match most requirements. In the event that it cannot be developed sufficiently in time for the instrument construction, several alternatives may be used to fill different imaging needs.

An imaging camera based on PImMS CMOS sensor is currently being developed at ISIS/RAL [Pooley 2017]. This detector is simple in several aspects, for instance not requiring vacuum to operate. It has been demonstrated in its intended final configuration but must yet be scaled to a larger area. The scaling is limited by wire bonds, resulting in at best a 22-mm wide stripe detector that must be translated in 1 dimension in order to cover a larger area of 100x100mm^2. This detector may be suitable for static images with high resolution and flux.

Detectors based on a phosphorescent screen viewed through a mirror by a Timepix optical camera can be used for large field-of-view applications with lower resolution [Losko 2021]. Cameras with the same principle using a commercial sCMOS imager are also capable of time-resolved measurements and can be used to cover some of the applications, similar to the imaging setup at the PSI [Kaestner 2011]. A gas detector with a micro-pattern readout, such as on the RADEN instrument at J-PARC can be yet another alternative.

An alternative to the MCP which still uses Timepix chips can be neutron-semiconductor converter coupled to the Timepix using bump bonding [Herrera 2018]. The R&D on this type of detector are still in the early stages, however, several candidate materials exist [Chica 2020, Doan 2015, Maity 2018]. If crystals of sufficient quality and size can be grown in the near future, it may be possible to build a detector with the position resolution at least equal to the pixel size of Timepix (55x55um) and potentially a very high rate capability. The detector scalability would also be good, provided good edge performance of the semiconductor.

4.3 MULTI-TUBE DETECTOR FOR BWAVES

BWAVES requires a compact ring of position sensitive detectors around its innovative velocity selector. ToF resolution and high efficiency for very cold neutrons (14.5 Å and longer) suggesting a detector with a small depth but high fill-factor and a transparent entrance window. The Monoblock Multi-Tube (MT) detector offers a performance improvement over a conventional tube LPSD array. The detector body is made of Al, which is significantly more transparent to neutrons than stainless steel. The fill factor and detection thickness uniformity are optimized with rectangular tubes, and the tubes can be made shallower – 4 mm instead of 8 mm in case of conventional round tubes. While the presence of these advantages is qualitatively clear, a simulation effort will be required in order to estimate the level of improvement in the final data.

In terms of mechanics, the MT detector is a monolithic cylinder with flanges on to and on the bottom. The conventional tube solution has a support structure of approximately the same shape as the entire MT. Considering that the MT does not require any support structure, mechanically, the two detectors occupy approximately the same spatial envelope. The number of tubes, and therefore readout channels can be the same in MT as for round tubes, however, the tube pitch and number can be customized freely in case of the MT. For example, using 6 units of 32-channel readout, 192 tubes with 9.8mm pitch arranged in a circle with 300 mm radius, form a convenient configuration. In comparison, using 8-mm tubes (an industry standard dimension), one arrives at 208 tubes, corresponding to 6 and a half units of readout.

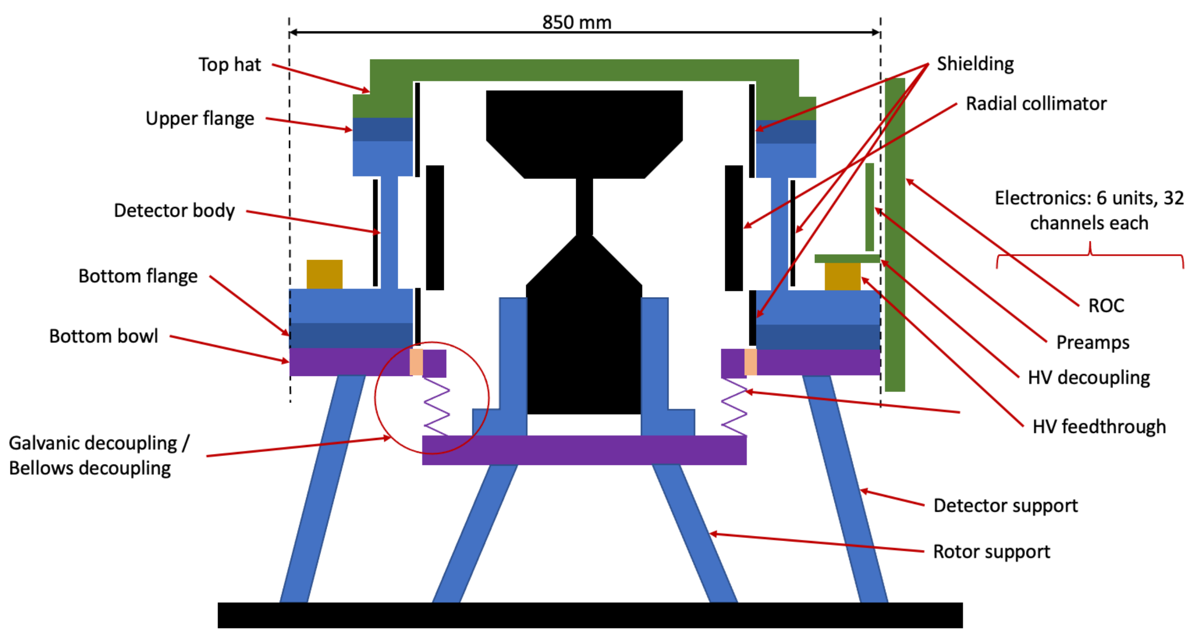

Concept of the detector and WAVES rotor vessel based on a Multi-Tube detector. The inner part (in black) is the WAVES device with the rotor at the top and the motor at the bottom.

A further innovative application of the MT detector can have the MT cylinder constitute the vertical section of the vacuum vessel. With top and bottom covers creating an interface to the sample and a high vacuum cavity for the WAVES-rotor, and, if required, a radial collimator, the access to the detector electronics becomes trivial – HV decoupling, preamplifiers and digitizers will be in air and easily accessible on the outside of the vacuum vessel, while the neutron window of the detector is in vacuum. This solution further minimizes the amount of material in vacuum that may contaminate the rotor. An R&D effort is required however, to ensure the compatibility of the WAVES rotor and its motor with the detector in terms of noise pick-up, grounding and vibrations. Dedicated testing would be needed to validate the solutions for the interface of these two devices. An engineering study of the stresses and deformations under vacuum will be required and will be used to optimize the dimensions of the detector body, the flanges and the interface with the sample environment.

The readout electronics will primarily rely on established NScD electronics solutions. We would collaborate with the ILL on the HV decoupling boards and development of the pre-amplifiers. A standard ROC board solution will handle the back-end readout, allowing for complete support in-house during operations.

4.3.1 Feasibility: Multi-Tube Detector for BWAVES

The Multi-Tube technology has been extensively used at the ILL, LLB, and ANSTO on 8 instruments with 50+ total years of operation so far, demonstrating good reliability of the detector. A completely circular detector would be new, however. Performance risks are not expected; indeed, significant performance gains are expected.

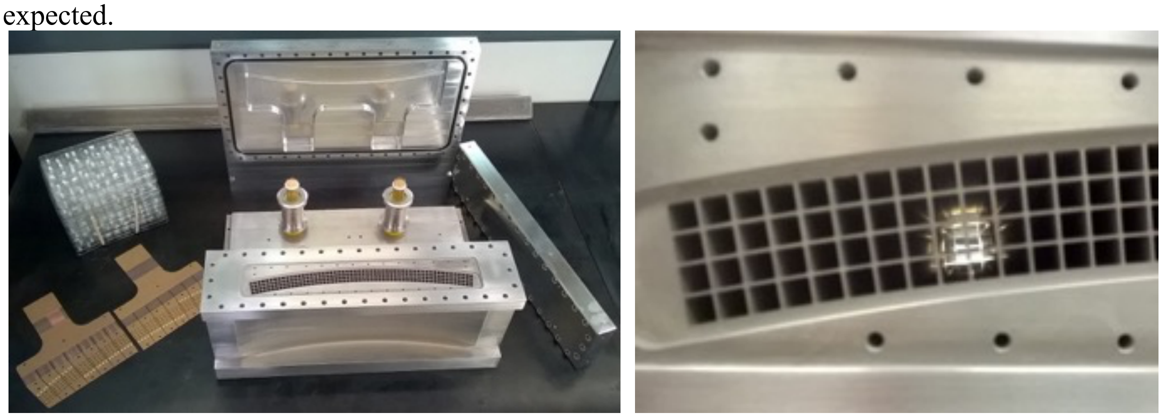

A curved Multi-Tube detector from the D3 instrument at the ILL. Left: the detector body and flanges. Right: closeup of the He3 tubes machined through the aluminum block.

4.3.2 Risks: Multi-Tube detector

Technological risk

- A circular Multi-Tube is new. It is possible that unknown issues complicate manufacturing.
- Mitigation: produce a prototype detector with desired curvature and tube dimensions.
- The detector faces the rapidly rotating WAVES device, whose failure modes are not yet known. If there is a possibility of puncture in the detector sensitive area, the entire detector body must be replaced (in case of conventional tubes, it may or may not be sufficient to replace only some of the tubes). The shock from the rotor breaking may cause anode wires to break.
- Mitigation: Simulate failure modes of the rotor. Include a spare detector body in the instrument scope. Transfer detector maintenance knowhow to the NScD detector team.

Schedule risk

- With the current schedule of instrument projects at STS and detector projects at the ILL, there is sufficient time to design, prototype, test, manufacture, and commission this detector.

Budget risk

- Cost of the detector body may be increased if a custom alloy/casting are required.
- Provision for spare components may need to included with the detector delivery.
- Mitigation: Early design study and cost estimates, early material procurement and testing. Include a spare detector body in instrument scope.

4.3.3 Opportunities: Multi-Tube

Beyond BWAVES main detector, future instruments requiring small ^{3}He tube dimensions with compact gaps and transparent neutron windows can benefit from the in-house MT knowledge. One potential application is a possible auxiliary detector on BWAVES that would be placed above the sample and the initial detector.

Additionally, a collaboration with the ILL to deliver this technology to ORNL opens for the possibility, both in terms of knowhow and in organizational terms, for future collaborations on other successful ILL ^{3}He detector technologies, such as the Trench-MWPC [Marchal 2017]. An existing in-house electronics solution with the adaptation for the MT detector, will make it easier to integrate these types of detectors if needed.

The option of Multi-Tube or a related detector technology on EXPANSE and VERDI is not out of question, but it is not currently considered to have a sufficiently strong driver. Instruments with curved detector geometry with sizes similar to BWAVES and up to about twice that size may benefit from the R&D on Multi-Tube at the ORNL.

Finally, beam monitors based on the Multi-Tube technology are currently in development and may present an adequate solution for measuring integrated ToF spectra of moderately intense beams. A common project could deliver both monitors are well as the BWAVES detector.

4.3.4 Back-up Solution: Multi-Tube

In case the Multi-Tube detector is found inappropriate due to an unforeseen reason, a conventional ^{3}He tube detector can be built instead. This would require separating the vacuum tank and the detector, requiring somewhat more space and a solution for electronics in vacuum. These points do not present an insurmountable challenge.

4.4 VACUUM-COMPATIBLE ANGER CAMERAS

R&D in developing a vacuum-compatible Anger camera detectors will enhance instrument performance by eliminating a window in front of the detector active element (scintillator) while keeping most detector electronics in air where it can be cooled and maintained. This removes the necessity of constructing vacuum-tight air enclosures surrounding the entire detector which complicate access to detector electronics, thus mitigating the risk of significant instrument downtime. The performance of CENTAUR will benefit from placing the detectors in vacuum in order to minimize scattering in inactive components. The Anger cameras proposed for CENTAUR have up till now not been operated in vacuum. A number of technical challenges need to be solved in order to enable this capability:

- The ROC boards must remain in air for cooling. While ROC boards have been placed in vacuum on instruments with ^{3}He detectors [Granroth 2006, Abernathy 2012], the electronics density is much higher on an array of Anger cameras, such as proposed on CENTAUR. Therefore, a camera can either be placed on a vacuum boundary – the sensor in vacuum and the electronics outside, or with an air-box around the electronics. In either case, the vacuum boundary needs to be incorporated into the camera design.
- The preamplifiers need to be very close to the SiPM to maintain signal integrity. Further, the sheer number of connectors between the SiPM and preamplifiers, make feeding out the SiPM signals to out-of-vacuum preamplifiers complicated. This will be looked at as a backup solution only. The preamplifiers are expected to be placed in vacuum.
- The temperature of the SiPM must be stable and repeatable to within 1°C. This is a challenge due to the low, but non-negligible heat produced in the preamplifiers.
- The x- and y-summed preamplifier signals must be fed out of vacuum. The number of leads is large, but not prohibitive.
- The Anger Camera must be on a floating ground, isolated from the vacuum vessel.
- There needs to be access to both vacuum and air portion of the Anger camera for maintenance and repair.
- The optical package – the scintillator and SiPM assembly – must be in a light-tight enclosure, yet this enclosure must be able to rapidly vent to vacuum during pump-down and fill with air during venting of the vacuum vessel. Failing this, the optical package would be (de)pressurized, causing stress or damage of the SiPM and movement of scintillator with respect to the SiPM.

4.4.1 Feasibility: Vacuum Anger Camera

While no one of the points above are trivial and all require a considerable R&D effort, each is feasible.

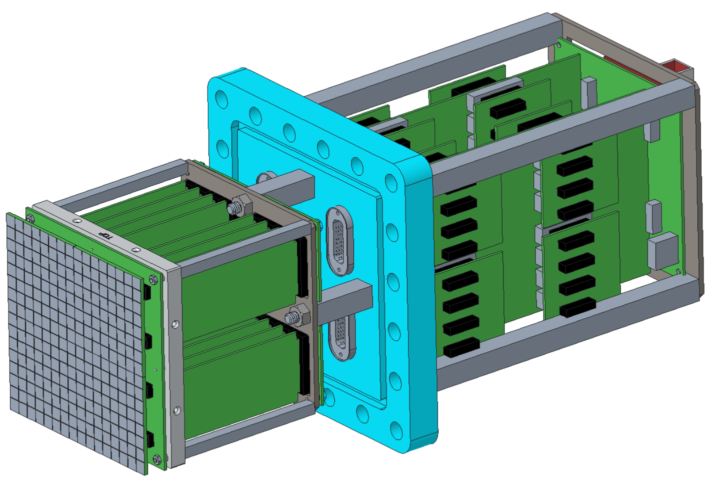

Concept of a vacuum Anger camera. From left to right: the SiPM and preamplifiers in vacuum, vacuum flange, digitizers in air.

4.4.2 Risks: Vacuum Anger Camera

Risks stem mainly from the application of multiple solutions simultaneously, in a design where space is limited as is the total acceptable dead area. Further, it is not predictable whether one or more of the above points may require significantly more effort than originally envisaged. An overarching risk mitigation is the fall back to in-air Anger cameras. For this reason, the design of the vacuum vessel will remain compatible with detectors in air until the in-vacuum solution will have been validated. An initial R&D effort to validate the feasibility of Anger cameras in vacuum is foreseen, followed by R&D leading to a prototype camera for CENTAUR.

Performance risk

- Even with a successful vacuum Anger camera implementation, the performance gain over the non-vacuum solution is insignificant.
- Other performance limitations may be created in the process of implementation, such as increased dead area, or increased sensitivity to electronic noise.
- Mitigation: Simulate expected instrument performance for cameras in air and vacuum. Design study of several possible vacuum and air configurations. In-beam test testing as a part of R&D.

Schedule risk

- Due to a large number R&D questions, the risk of at least one taking much longer than expected is considerable.
- Mitigation: Early design study, prototyping at essential milestones. Vacuum testing of prototypes.

Budget risk

- Many additional vacuum-compatible components need to be used: off-the-shelf, and bespoke both. Prices and manufacturing costs may not be known until the final design is defined, including grade of each component.
- Mitigation: Early design study, prototyping.

4.4.3 Opportunities: Vacuum Anger Cameras

Many neutron scattering instruments call for an evacuated neutron flight path between sample and detector. Up till now, this could only be achieved with ^{3}He detectors. With other detectors, a vacuum, or Ar- or He-filled box had to be used, with the detectors measuring neutrons through a window. With the availability of a vacuum solution, high signal-to-noise instruments with high special resolution become possible.

4.4.4 Back-up Solution: Vacuum Anger Camera

In case an in-vacuum solution cannot be achieved, or requires significant trade-offs, the detectors will be placed in a more conventional fashion, outside of the vacuum vessel, registering incoming neutrons through an aluminum vacuum window. This configuration has been demonstrated on TOPAZ and MANDI and does not present a technological challenge for detectors.

4.5 HIGH-RESOLUTION ANGER CAMERA

Position resolution of 0.2-mm (in at least one dimension) is required for SEMSAMS implementation on CENTAUR. This is currently difficult to achieve with most types of detectors. While a WLSF detector can reach this resolution, an Anger camera offers a large increase in rate capability, provided it’s position resolution can be enhanced to meet the 2-mm requirement.

Position resolution of an Anger camera depends on the physical pixel size or pitch of the sensor used as well as on the light yield of the scintillator. In the NScD implementation, the camera resolution is approximately 10 times better than the SiPM pixel pitch [Riedel 2015], provided that the scintillator thickness has been optimized for resolution. SiPMs with pixel pitch of 7.2, 6.4 and 3.36 mm have been tested and show corresponding position resolutions 0.6, 0.5 and 0.35mm. Further decrease of the pixel size, however, does not result in better position resolution, as the light yield of the scintillator becomes the limiting factor. Position resolution of 0.2mm may be achieved using a brighter scintillator with 3-mm SiPM pixels. Suitable scintillators exist but are either difficult to use, such as LiI, or have not yet been produced in sufficient quality commercially. LiI is a highly hygroscopic material and therefore must be permanently sealed at the time of production.

Replacing the SiPMs in the Anger camera with a more finely pixelated ones would result in a camera where the optical package was narrower than the electronics. This would preclude it from being used as a unit in a continuous array, however, it can still be used to for occasional SEMSANS experiments, temporarily replacing the 0-degree camera. It may also be possible to offset the optical packages of the neighbor Anger Camas to partially close the gap. Further R&D may be able to achieve correspondingly more compact electronics.

4.5.1 Feasibility: High-Resolution Anger Camera

It is known that with a bright scintillator, the required position resolution can be achieved with an appropriate SiPM sensor. Encapsulated LiI may work. It is a known scintillator for neutron detection, and a reasonable R&D effort can be expected to achieve encapsulation. A variety of newer scintillators have been under investigation over the past decades [Wang 2018, Boatner 2017]. One of these may work if LiI does not.

4.5.2 Risks: High-Resolution Anger Camera

In terms of the sensor integration and the electronics package, the proposed high-resolution camera is a modification of an existing design with alternative components, therefore only a low level of risk is expected. There are unknowns with the scintillator, however.

Performance risk

- The R&D on LiI, and other potential scintillators do not yield a reliable product.
- Long-term scintillator performance may degrade due to imperfect encapsulation.
- Mitigation: backup solution for SEMSANS; multiple scintillator options in R&D.

4.5.3 Opportunities: High-Resolution Anger Cameras

An Anger camera with a 0.2 mm position resolution may be useful in other applications. This position resolution is not achieved with many types of detectors. It may be sufficient for imaging with relaxed resolution. There may be R&D synergies with the SiPM pixel camera, which is also intended to use SiPMs with small pixels.

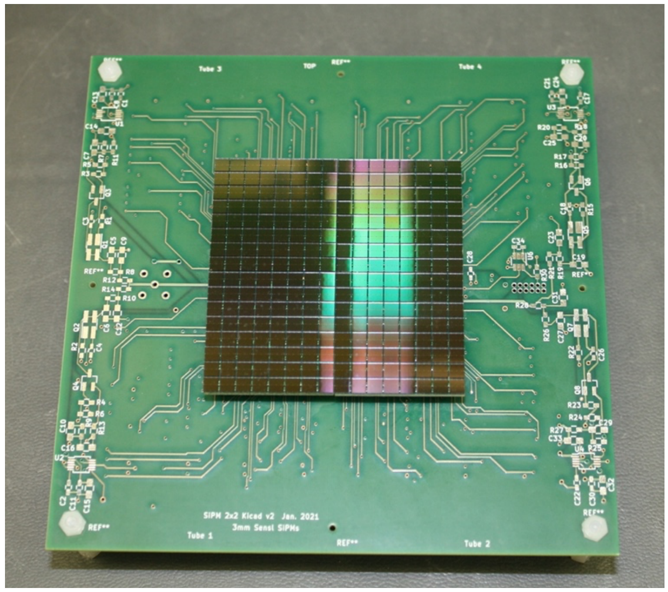

2x2 SiPM 8x8 pixel arrays with 3-mm pixel pitch. The PCB is designed to match the size of electronics for a camera with 7-mm pixels.

4.5.4 Back-up Solution: High-Resolution Anger Camera

A 1-D wavelength-shifting fiber detector, such as the one used for SEMSANS on LARMOR, ISIS, achieves the required position resolution. Both ORNL and ISIS have experience with WLSF detector technology and there are no barriers expected to realize such a detector as a back-up. It would, however, be rate-limited, and may require 1 to 2 orders of magnitude of beam attenuation.

5. NEUTRON BEAM MONITORS

Beam monitors serve several purposes on a beam line, providing information for, but not limited to:

- Data normalization
- Time-of-Flight corrections
- Diagnostics of chopper performance
- Diagnostics of guide performance
- Diagnostics of moderator performance
- Verification of beam profile on sample

Beam monitors are invaluable during the commissioning phase of an instrument, however, use of beam monitors presents trade-offs. A monitor invariably represents additional material in beam. Relatively transparent monitors exist, but even these will attenuate on the order of 1 to a few percent. Position-sensitive monitors, generally, will have more attenuation than non-position-sensitive versions [Issa 2017]. Similar to other beam windows, the attenuation is wavelength dependent. In particular, wavelengths corresponding to Bragg edges will be attenuated more than other wavelengths.

Counting rate in a monitor must be kept at a level where the counts have a sufficient statistical significance, in particular to reconstruct a ToF spectrum. On the other hand, like any other detectors, they should not saturate. This means that the efficiency must be carefully selected. This may be a challenge, if a monitor is to measure very different beam settings, such as high-resolution vs. high-flux.

5.1 BEAM MONITOR PERFORMACE ISSUES

Beam monitor technology can be greatly improved in two ways: increase of dynamic range, and improvement of material budget, or transparency, in position-sensitive monitors.

5.1.1 Beam Monitor Dynamic Range

Depending on the setting of an instrument, such as incident energy, collimation and energy resolution, a monitor may see fluxes that vary by many orders of magnitude. In order to not saturate at high rate and at the same time to collect sufficient statistics at low rate, efficiency, the speed of the monitor, electronics and the sensitivity to background must be carefully balanced.

An increase in the maximum rate capability is desired. At the lower end of the dynamic range, background will impose limits. As an example, in a ^{3}He chamber monitor, low efficiency can be reached by using a very small pressure of ^{3}He mixed with a normal pressure of a quenching gas, ex. $ArCO_2$. When a ^{3}He tube is used as a high-efficiency neutron detector, the number of interactions in the detector is dominated by neutron conversions in ^{3}He due to its large thermal neutron cross section. However, as ^{3}He pressure is drastically lowered, say by a factor 10^6, the cross sections of Ar, Al, and other elements present in the monitor to gamma-rays and fast neutrons become greater than thermal neutron cross section. A low-efficiency monitor may be more sensitive to gamma-rays and fast neutrons, than to thermal neutrons. This is an issue especially close to the source, where direct radiation from the target may propagate along the guide and may be generated by secondary nuclear reactions in the beam line.

Furthermore, achieving very low efficiency via a very low concentration of the converter isotope with any accuracy is difficult. This would involve a few ubar of ^{3}He, or a few nm of coating in case of a ^{10}B detector.

The preferred option is therefore to increase the rate capability of the monitors. Up to a neutron efficiency of about 1%, the beam monitor efficiency can be increased without raising the attenuation beyond what is in most cases already present due to the monitor housing.

A potential method to increase the dynamic range is to combine monitors of different efficiencies in a single package. For instance, Cascade Detector Technologies (CDT) have proposed a Gas Electron Multiplier (GEM) monitor with two ^{10}B layers each with a separate readout. Depending on the flux, the more appropriate of the monitors is chosen, while the other is powered down. The material budget of the monitor need not increase significantly with this addition (in case of the GEM monitor, the main absorber is the anode readout plane which is common for both ^{10}B layers).

5.1.2 Transparency of Beam Monitors

While beam-integrating monitors can be built with relatively little material, position-sensitive monitors tend to have a readout structure of some type that introduces further material into the beam. In some cases, the monitor may be translated out of the beam for the majority of measurements and inserted into the beam only during diagnostics. If mechanically and practically acceptable, this is a good option that leaves useful beam unperturbed.

5.1.3 Beam Monitor Stability and Linearity

A beam monitor is required to be stable over time to be truly useful. This is often a challenge because components of a monitor age due to radiation exposure. Even at a moderate neutron detection rate, the exposure to gamma rays and fast neutrons, may degrade the performance. Linear response vs. neutron flux is necessary to accurately normalize the experimental data. In practice, this frequently limits the usefulness of a monitor.

5.2 BEAM MONITOR R&D

Neutron beams at a high-brightness source, such as the STS, transport up to 10^{10} neutrons per second through a cross section of only a few cm^2. At various positions along a beamline, neutron intensity will vary greatly depending on chopper, collimation, polarization and other beam conditioning settings. The STS instruments rely on Time-of-Flight to operate correctly. Diagnosing and monitoring correct time distribution along a beamline is a major goal for beam monitors. This means monitoring the intensity as choppers open and close, and monitoring as the peak flux (around 2Å) turns into the minute, yet highly desirable flux at very long wavelengths (ex. 25Å, in instruments using 7.5Hz operation). There is currently no likely candidate for a monitor that can simultaneously collect useful statistics over the relevant dynamic range of neutron fluxes and do so without significant attenuation of the beam. It is therefore proposed to focus R&D on engineering solutions for translation of monitors in an out of beam. For locations where translation is undesirable, the compromise in performance must be made, prioritizing either flux or spectroscopic measurement and performance versus attenuation. Commercial solutions, and proven techniques from facilities around the world – with appropriate customization – may be used for translating, or fixed monitors.

5.2.1 Translating Beam Monitors

The design of a beam monitor is typically that of a slim box to be placed across the beam [Issa 2017]. Most gas-filled monitors have 1 bar internal pressure. A scintillation monitor may have vacuum inside or be filled with air. In cases where the guide vacuum has an interruption due to other reasons, a monitor may be placed on a translation stage and moved in and out of the beam as needed.

For placing a monitor inside the guide vacuum, it's windows may need to be reinforced to withstand the pressure differential. This will increase attenuation by a few percent, however, since the monitor is removed from the beam during experiments, this is acceptable. It is indeed preferable compared to placing the monitor in air, since for operation, there will be no material in beam. A translation stage in vacuum must fulfil the following:

- Must accommodate motion in vacuum with high reproducibility.
- Must feed through signals, high voltage, low voltage and/or gas supply.
- Must galvanically isolate the monitor and its cables from the beamline.
- Must not interfere with adjacent components.
- Must minimize the interruption of the guide

Beam monitors too have to be modified for compatibility with the translation stage. This is expected to be feasible – most beam monitor manufacturers provide custom solutions and are open to co-design towards a specific application.

5.2.1.1 Risks: translating beam monitors

Performance, operational risks

- Failure of the mechanical components in operation.
- Failure scenarios where a monitor stops half-way into the beam.
- Highly scattering monitors may create background for the neighbor beamlines

Mitigations

- Design to fail with monitor out of the beam. Provide an access path to monitors and their translation mechanisms.
- Design to prevent failure where a monitor stops part-way into the beam. Build in manual overrides.
- Simulate shielding performance including the monitor scattering as a radiation source. Increase local shielding around the monitor (it may be sufficient to cover the housing of the translation stage with borated sheets/panels).

5.2.1.2 Opportunities: translating beam monitors

Integrating translating monitors potentially increases the benefits of monitor data available for an experiment, without a significant investment into beam monitor R&D. It allows to use the best technological solutions that would otherwise have to be truncated to meet the transparency requirement.

The solution is versatile. When motivated, the instrument can be operated with all monitors in beam, accepting significant beam loss and background increase. This can be done in select few user beamtimes, but primarily for diagnostics and set-up.

5.2.2 Beam Monitor Development and Validation

Commercial solutions and adaptation of existing monitors can be used for both translating and fixed monitors. Provisions must be made for co-design with suppliers and testing of beam monitors with regards to performance in beam as well as for mechanical, electronic and data chain integration. Depending on the choice of monitor technology, in-house design and assembly may need to be foreseen. Following types of monitors are of interest for the STS, however a limited selection will be made in order to standardize the equipment as much as possible while addressing the requirements.

- Scintillator / optical fiber monitors. Used extensively at ISIS, this type of monitor has the lowest beam attenuation. While it does not fully integrate the beam, it does provide ToF spectra useful for many diagnostics. A drawback is gamma sensitivity and lack of radiation hardness in the current implementation.
- ^{10}B ionization chambers. Counting ionization chambers have recently been offered by CDT. It remains to be seen whether these monitors perform as claimed. If so, they may present an adequate solution for extreme environments, such as the bunker.
- ^{235}U ionization chambers. Fission chambers of efficiencies between 10^{-7} and 10^{-3} are available from LND, Inc. These, unfortunately, have high and irregular attenuation and poor uniformity [Lafont 2020, Issa 2017]. The fission reaction liberates fast neutrons in addition to the fission fragments, making it inappropriate in background-sensitive areas, such as in instrument caves. An advantage is the greatest neutron/gamma discrimination of any type of detector.
- GEM ^{10}B monitors are manufactured by CDT, among others. These have position sensitivity and a much higher rate capability compared to other monitor types. Unfortunately, the presence of the GEM foil and the readout structure in the beam lead to considerable attenuation. This suggests translating GEM monitors in and out of the beam.
- $^{3}He/^{14}N_2/^{10}B$ proportional counters – the most common type of monitor that builds on the successful principle of the ^{3}He tube. Unfortunately, removing the benefit of the exceptional efficiency of ^{3}He, leaves very little in the way of advantages of this type of monitors.
- Multi-Tube monitors are currently in development at the ILL. Based on the same principle as the Multi-Tube detector, this monitor divides the incoming flux over a set of tubes with fast charge collection, significantly increasing rate capability and gamma rejection. It may also be configured with limited position sensitivity.

The following beam monitor technologies are proposed depending on locations:

- Bunker: ionization chambers (fixed), Multi-Tube (translating), scintillator (translating, shielded).
- Guide: Multi-Tube (translating), GEM (translating), scintillator (fixed).
- Cave: Multi-Tube (translating/fixed), GEM (translating), scintillator (fixed).

5.3 NEUTRON CAMERAS

Imaging the beam is essential for ensuring correct beam distribution and focusing at the sample position. It may also be relevant to image either the transmitted beam after the sample, or slightly upstream of the sample. A camera differs from a position sensitive monitor in that it is not expected to be transparent for the beam, the accent is instead on high position resolution. The camera is removed during sample measurement and may be shared between multiple instruments.

5.3.1 Neutron Camera R&D

It is expected that stand-alone commercial solutions will be available in time for first beam at STS. Mechanical, electronic, and data integration will require in-house effort. Synergies with the imaging beamline R&D can be leveraged. It is possible that a smaller scale, or a lower efficiency version of imaging detectors will make an excellent neutron camera for beam imaging purpose.

6. DETECTOR R&D MILESTONES

This section presents the milestones, scope of work, resources and timeline for the detector R&D work described in section 4. The parts of the tables shown in grey refer to the work beyond the R&D scope, within the instrument construction scope to complete the corresponding detector delivery.

6.1 SiPM PIXEL DETECTOR

Milestone	Scope of Work	Main Contributions	Needed by
1x1 mm^2 pixel scintillator	Produce 32x32-pixel scintillator, 1x1 mm^2 pixels	Vendor	1 year before end of Preliminary design, QIKR, mid 2024 (CY)
Detector scaled to 100x100 mm^2	Design electronics for a 6x6 SiPM array (105x105 mm^2)	STS, NScD	1.5 years before end of final design, QIKR
	Build 48x48 pixel GS20 scintillator (3x3 array of 16x16 pixels)	STS, NScD	
	Purchase components and assemble detector, test in beam.	STS, NScD	
100x100 mm^2 detector characterized	Performance report: rate, gamma sensitivity (2-mm, 1-mm pixels), reflectometer performance, ageing.	STS	End of final design, QIKR
	Choose components, choose scintillator parameters.	STS	
	Preliminary design 200x200 mm^2 detector.	STS	
Final detector (200x200 mm^2)	Final design 200x200 mm^2 detector	STS	During procurement, QIKR
	Purchase components	STS	
	Assemble detector, test in beam.	STS	
Deliver QIKR Detector	Install on QIKR, commission	STS	End of construction, QIKR

6.2 IMAGING DETECTOR

Milestone	Scope of Work	Main Contributions	Needed by
Timepix4 development plan	Develop vs. Outsource	STS, Collaboration / Contractor	2022 (early in CUPI2D preliminary design)
Timepix4 (1x1) demonstrated	Bond Timepix4	Contractor / Collaboration	End of CUPI2D preliminary design (approximate – some time before MCP, semiconductor milestones)
	Timepix4 firmware, readout	Contractor / collaboration	
	Timepix4 test with current MCP (28x28 mm^2)	STS, NScD	
	DAQ chain prototype	STS, NScD, Contractor / collaboration,	
Timepix4 2x1+ array	Electronic design, Firmware design	STS, NScD / Collaboration	End of final design, CUPI2D
	Mechanical design – adapt 28x28 mm^2 MCP	STS	
	Procurement, assembly in-beam test.	STS, NScD	
	DAQ chain	STS, NScD, Contractor / Collaboration	
MCP 100x100 mm^2 demonstrated	Characterize large MCPs from Nova using Timepix3	NScD	End of final design, CUPI2D
	MCP production plan	Vendor, STS, NScD	
Semiconductor converter demonstrated	Demonstrate and characterize with 1x1 Timepix(3 or 4)	STS, NScD / collaboration	End of final design, CUPI2D
	Manufacture, bond semiconductor across chip boundary (up to 2x2, 56x56 mm^2 semiconductor)	Vendor / Collaborator	
MCP 100x100 mm^2 produced	Produce 100x100 mm^2 MCP	Vendor	End of Procurement, CUPI2D
	Test with 4x4 Timepix4	STS, NScD, Collaboration / Contractor	

Full scale semiconductor converter	Manufacture, bond a 4x4 (100x100 mm^2 semiconductor)	Vendor / Collaborator	End of procurement, CUPI2D
100x100 mm^2 detector	Detailed design	STS	End of construction, CUPI2D
	Procure, Assemble	STS	
	Install, commission	STS	

6.3 MUILTI-TUBE DETECTOR

Milestone	Scope of Work	Main Contributions	Needed by
MT Preliminary Design	Define geometry of MT detector	STS, Collaboration	1.5 years before end of BWAVES preliminary design, end of 2023 (CY)
	Simulate MT performance on BWAVES	STS	
MT Prototype	Define prototype	STS, Collaboration	1 year before end of Final Design BWAVES
	Design prototype	STS, Collaboration	
	MT tooling at STS	STS	
	MT STS electronics	NScD, Collaboration	
	Procure, assemble, FAT	Collaboration	
	Validate Al background	Collaboration, STS	
	SAT, in-beam test, Report	STS	
BWAVES Detector manufactured	MT detailed design	Collaboration, STS	End of procurement, BWAVES
	Procure Al	Collaboration	
	Procure, manufacture and assemble	Collaboration	
	FAT	Collaboration, STS	
BWAVES detector installed	SAT	STS	End of construction, BWAVES
	Installation, Commissioning.	STS	

6.4 VACUUM ANGER CAMERA

Milestone	Scope of Work	Main Contributions	Needed by
Vacuum AC proof-of-principle	Design test vacuum chamber	STS	1.5 years before end of CENTAUR preliminary design, end of 2023 (CY)
	Assemble AC for vacuum testing	STS, NScD	
	Test pump down, cooling, n detection	STS, NScD	
	Performance simulation	STS	
	Preliminary design	STS	
CENTAUR detector prototype	Electronics, mechanical design	STS	End of Final design, CENTAUR
	Scintillator area test	STS, NScD	
	Procurement, assembly, in-beam test	STS	
CENTAUR detectors produced	Final design	STS	End of procurement, CENTAUR
	Procurement, assembly, in-beam tests	STS, NScD	
CENTAUR Detectors delivery	Installation, Commissioning	STS	End of construction, CENTAUR

6.5 HIGH-RESOLUTION ANGER CAMERA (SEMSANS)

Milestone	Scope of Work	Main Contributions	Needed by
SEMSANS Prototype	Short-list suitable scintillators	STS, NScD	End of preliminary design, CENTAUR
	Test scintillators with existing 3-mm SiPM pixel AC	STS, NScD	
	Borofloat or other glass enriched in B-10	Vendor	
	Select scintillator, report	STS	

CENTAUR 0-deg Detector Preliminary Design	Preliminary design 0-deg detector	STS	Start of final design, CENTAUR
Deliver CENTAUR 0-deg detector	Detailed design	STS	End of procurement, CENTAUR
	Electronics design	STS, NScD	
	Procurement, assembly	STS	
	Installation, commissioning	STS	

7. REFERENCES

[Marchal 2021] Marchal, J. et al., *First measurements with the new ^{3}He-filled Monoblock Aluminium Multitube neutron detector developed at the ILL for ANSTO PLATYPUS reflectometer*, J. of Neutron Research 23 (2021) 53–67, DOI 10.3233/JNR-200179

[Khaplanov 2013] Khaplanov, A. et al., *Investigation of gamma-ray sensitivity of neutron detectors based on thin converter films*, 2013 JINST 8 P10025 doi:10.1088/1748-0221/8/10/P10025

[Mauri 2019] Mauri, G., et al., *Fast neutron sensitivity for ^{3}He detectors and comparison with Boron-10 based neutron detectors*, Mauri et al. EPJ Techniques and Instrumentation (2019) 6:3 https://doi.org/epjti/s40485-019-0052-x

[Khaplanov 2017] Khaplanov, A. et al., *Multi-Grid detector for neutron spectroscopy: results obtained on time-of-flight spectrometer CNCS*, 2017 JINST 12 P04030, doi:10.1088/1748-0221/12/04/P04030

[Bewley 2011] Bewley, R.I. et al., *LET, a cold neutron multi-disk chopper spectrometer at ISIS*, NIM A 637 (2011) 128–134, doi:10.1016/j.nima.2011.01.173

[Olivier 2010] Olivier, J. et al., *The New Cold Neutron Time-of-Flight Spectrometer IN5*, (2010) Neutron News, 21: 2, 22 — 25, DOI: 10.1080/10448631003757573

[Riedel 2015] Riedel, R.A. et al., *Design and performance of a large area neutron sensitive anger camera*, NIM A 794 (2015) 224–233, http://dx.doi.org/10.1016/j.nima.2015.05.026

[Marchal 2017] Marchal, J. et al., *Characterisation of a neutron diffraction detector prototype based on the Trench-MWPC technology*, 2017 JINST 12 C12009, https://doi.org/10.1088/1748-0221/12/12/C12009

[Chong 2019] Chong, S.-A. et al., *High Data-Rate Neutron-Sensitive Pixelated Detector Using Silicon Photomultiplier*, 2019 IEEE (NSS/MIC), DOI: 10.1109/NSS/MIC42101.2019.9059763

[Chong 2021] Chong, S.-A. et al., *The development of a 6Li-based pixelated neutron detector for neutron reflectometry at the Spallation Neutron Source*, submitted to NIM A

[Huq 2019] Huq, A. et al., *POWGEN: rebuild of a third-generation powder diffractometer at the Spallation Neutron Source,* J. of Applied Crystallography 2019 Journal Volume: 52 Journal Issue: 5; ISSN 1600-5767

[Maliszewskyj 2018] Maliszewskyj, N. J. et al., *An energy analyzing detector for cold neutrons*, NIM A 907, (2018), 90-96, https://doi.org/10.1016/j.nima.2018.05.023

[Richards 2021] Richards, S. et al., *High count rate pulse shape discrimination algorithms for neutron scattering facilities*, NIM A 989, (2021), 164946, https://doi.org/10.1016/j.nima.2020.164946

[Sykora 2018] Sykora, J. et al., *ZnO:Zn/^{6}LiF scintillator—A low afterglow alternative to ZnS:Ag/^{6}LiF fort hermal neutron detection*, NIM A 883, (2018), 75-82, https://doi.org/10.1016/j.nima.2017.11.052

[Wang 2016] Wang, C. L. et al., *Performance improvements of wavelength-shifting-fiber neutron detectors using high-resolution positioning algorithms*, Rev. of Scientific Instruments 87, 053303 (2016); https://doi.org/10.1063/1.4949496

[Wang 2015] Wang, C. L. et al., *Optimizing ZnS/6LiF scintillators for wavelength-shifting-fiber neutron detectors, 2015 IEEE (NSS/MIC)*, 2015, pp. 1-6, doi: 10.1109/NSSMIC.2015.7581839.

[Tremsin 2020] Tremsin, A. S. and J.V.Vallerga, *Unique capabilities and applications of Microchannel Plate (MCP) detectors with Medipix/Timepix readout*, Rad. Measurements Volume 130, January 2020, 106228, https://doi.org/10.1016/j.radmeas.2019.106228

[Berry 2013] Berry K. D. et al., *A Neutron Sensitive Microchannel Plate Detector with Cross Delay Line Readout, 2012 IEEE (NSS/MIC)*, 2012, pp. 192-198, doi: 10.1109/NSSMIC.2012.6551091

[Khaplanov 2015] Khaplanov, A. et al., *Investigation of background in large-area neutron detectors due to alpha emission from impurities in aluminium*, 2015 JINST 10 P10019, doi:10.1088/1748-0221/10/10/P10019

[Zanini, 2020] Zanini, L. et al., *Neutronic Design of the Bunker Shielding for the European Spallation Source*, J. of Surface Investigation: X-ray, Synchrotron and Neutron Techniques, 2020, Vol. 14, Suppl. 1, pp. S251–S253. DOI: 10.1134/S1027451020070538

[Santoro 2018] Santoro, V. et al., *Study of neutron shielding collimators for curved beamlines at the European Spallation Source*, arXiv:1804.02889v1

[Rossi 2015] Rossi, E., *Characterisation of the Spatial Resolution and the Gamma-ray Discrimination of Helium-3 Proportional Counters*, Master's Thesis, U. of Milano-Bicocca (2015), arXiv:1702.06501v2

[Wang, Riedel 2016] Wang, C. L. and Riedel, R. A., *Improved neutron-gamma discrimination for a 6Li-glass neutron detector using digital signal analysis methods*, Review of Scientific Instruments 87, 013301 (2016); https://doi.org/10.1063/1.4939821

[Stefanescu 2017] Stefanescu, I. et al, *Neutron detectors for the ESS diffractometers*, 2017 JINST 12 P01019, doi:10.1088/1748-0221/12/01/P01019

[Chapon 2011] Chapon, L. C. et al., *Wish: The New Powder and Single Crystal Magnetic Diffractometer on the Second Target Station*, Neutron News, 22:2, 22-25 (2011), DOI: 10.1080/10448632.2011.569650

[Ankner 2008] Ankner J.F. et al., *The SNS liquids reflectometer*, Neutron News, 19, 3, 14 (2008).

[Campbell 2011] Campbell, R. A. et al, *FIGARO: The New Horizontal Neutron Reflectometer At The ILL*, European Physical Journal Plus, 2011, 126, 107

[Wang 2018] Wang, C. L. et al, *Bright Eu2+-activated polycrystalline ceramic neutron scintillators*, NIM A 883 (2018) 1–8, https://doi.org/10.1016/j.nima.2017.11.013

[Boatner 2017] Boatner, L. A. et al, *Improved lithium iodide neutron scintillator with Eu2+ activation: The elimination of Suzuki-Phase precipitates*, NIM A 854 (2017) 82–88

[Piscitelli 2018] Piscitelli, F. et al., *Characterization of the Multi-Blade ^{10}B-based detector at the CRISP reflectometer at ISIS for neutron reflectometry at ESS*, 2018 JINST 13 P05009, https://doi.org/10.1088/1748-0221/13/05/P05009

[Mauri 2020] Mauri, G. et al., *The Multi-Blade Boron-10-based neutron detector performance using a focusing reflectometer*, 2020 JINST 15 P03010, https://doi.org/10.1088/1748-0221/15/03/P03010

[Andersen 2020] Andersen, K. H. et al, *The instrument suite of the European Spallation Source*, NIM A, Volume 957, 21 March 2020, 163402, https://doi.org/10.1016/j.nima.2020.163402

[Pooley 2017] Pooley, D. E. et al., *Development of the "GP2" Detector: Modification of the PImMS CMOS Sensor for Energy- Resolved Neutron Radiography*, IEEE Trans. On Nuclear Science, vol. 64, NO. 12, 2017

[Parker 2018] Parker, J. D. et al., *Development of Energy-Resolved Neutron Imaging Detectors at RADEN*, JPS Conf. Proc. 22, 011022 (2018), https://doi.org/10.7566/JPSCP.22.011022

[Parker 2017] Parker, J. D. et al., *Counting-type Neutron Imaging Detectors at RADEN/BL22*, Hamon (online) Vol.27, No.1 2017

[Kaestner 2011] Kaestner, A. P. et al., *The ICON beamline – A facility for cold neutron imaging at SINQ*, NIM A 659 (2011) 387–393, doi:10.1016/j.nima.2011.08.022

[Losko 2021] Losko, A. A. et al., *New perspectives for neutron imaging through advanced event-mode data acquisition*, Scientific Reports (2021) 11:21360, https://doi.org/10.1038/s41598-021-00822-5

[Granroth 2006] Granroth, G. E. et al., *SEQUOIA: A fine resolution chopper spectrometer at the SNS*, Physica B 385–386 (2006) 1104–1106, doi:10.1016/j.physb.2006.05.379

[Abernathy 2012] Abernathy, D. L. et al., *Design and operation of the wide angular-range chopper spectrometer ARCS at the Spallation Neutron Source*, Rev. Sci. Instrum. 83, 015114 (2012); doi: 10.1063/1.3680104

[Herrera 2018] Herrera, E. et al., *Neutron Imaging with Timepix Coupled Lithium Indium Diselenide*, J. Imaging 2018, 4, 10; doi:10.3390/jimaging4010010

[Chica 2020] Chica, D. G. et al., *Direct thermal neutron detection by the 2D semiconductor $^{6}LiInP_2Se_6$* Nature | Vol577 | 16January2020, https://doi.org/10.1038/s41586-019-1886-8

[Doan 2015] Doan, T.C. et al., *Hexagonal boron nitride thin film thermal neutron detectors with high energy resolution of the reaction products*, NIM A, Volume 783, 21 (2015), 121-127, https://doi.org/10.1016/j.nima.2015.02.045

[Maity 2018] Maity, A. et al., *Hexagonal boron nitride neutron detectors with high detection efficiencies*, J. Appl. Phys. 123, 044501 (2018); https://doi.org/10.1063/1.5017979

[Marchal 2017] Marchal, J. et al., *Characterisation of a neutron diffraction detector prototype based on the Trench-MWPC technology*, 2017 JINST 12 C12009, https://doi.org/10.1088/1748-0221/12/12/C12009

[Issa 2017] Issa, F. et al., *Characterization of thermal neutron beam monitors*, Phys. Rev. Accel. Beams 20, 092801 – Published 26 September 2017, https://doi.org/10.1103/PhysRevAccelBeams.20.092801

[Lafont 2020] Lafont, F. et al., *Uniformity of response of Uranium fission chambers used as neutron beam monitors*, 2020, arXiv:2111.13535

Leighton Coates

Digitally signed by Leighton Coates
Date: 2022.01.27 13:05:33 -05'00'